

1 Cost Effective Off-Grid Automatic Precipitation Samplers for 2 Pollutant and Biogeochemical Atmospheric Deposition

3
4 Alessia A. Colussi^{1,†}, Daniel Persaud^{1,†}, Melodie Lao¹, Bryan K. Place^{2,‡}, Rachel F.
5 Hems^{2,§}, Susan E. Ziegler³, Kate A. Edwards^{4,‡}, Cora J. Young^{1,2}, and Trevor C.
6 VandenBoer^{1,3}

7
8
9 ¹ Department of Chemistry, York University, Toronto, ON

10 ² Department of Chemistry, Memorial University, St. John's, NL

11 ³ Department of Earth Science, Memorial University, St. John's, NL

12 ⁴ Canadian Forest Service, Natural Resources Canada, Corner Brook, NL

13
14 [†] AAC and DP contributed equally to this work and have the right to list themselves as first author.

15 [‡] Now at: SciGlob Instruments & Services LLC, Columbia, MD, USA

16 [§] Now at: Department of Chemistry and Biochemistry, Oberlin College and Conservatory, OH, USA

17 [†] Now at: Climate Change Impacts and Adaptation Division, Lands and Minerals Sector, Natural Resources Canada, Ottawa, ON

18
19 **Correspondence:** Trevor VandenBoer (tvandenb@yorku.ca)

20 21 22 23 **Abstract**

24 An important transport process for particles and gases from the atmosphere to aquatic and
25 terrestrial environments is through dry and wet deposition. An open-source, modular, off-grid, and
26 affordable instrument that can automatically collect wet deposition samples allows for more
27 extensive deployment of deposition samplers in fieldwork and would enable more comprehensive
28 monitoring of remote locations. Precipitation events selectively sampled using a conductivity
29 sensor powered by a battery-based supply are central to off-grid capabilities. The prevalence of
30 conductive precipitation - that which initially contains high solute levels and progresses through
31 trace level concentrations to ultrapure water in full atmospheric washout, depends on the sampling
32 location but is ubiquitous. This property is exploited here to trigger an electric motor via limit
33 switches to open and close a lid resting over a funnel opening. The motors are operated via a
34 custom-built and modular digital logic control board, which have low energy demands. All
35 components, their design and rationale, and assembly are provided for community use. The
36 modularity of the control board allows operation of up to six independent wet deposition units,

37 such that replicate measurements (e.g., canopy throughfall) or different collection materials for
38 various targeted pollutants can be implemented as necessary.

39 We demonstrate that these platforms are capable of continuous operation off-grid for integrated
40 monthly and bimonthly collections performed across the Newfoundland and Labrador Boreal
41 Ecosystem Latitudinal Transect (47° to 53° N) during the growing seasons of 2015 and 2016.
42 System performance was assessed through measured power consumption from 115 volts of
43 alternating current (VAC; grid power) or 12 volts of direct current from battery supplies during
44 operation under both standby (40 or 230 mA, respectively) and in-use (78 or 300 mA, respectively)
45 conditions. In the field, one set of triplicate samplers was deployed in the open to collect incident
46 precipitation (open fall) while another set was deployed under the experimental forest canopy
47 (throughfall). The proof-of-concept systems were validated with basic measurements of rainwater
48 chemistry including: i) pH ranging from 4.14 to 5.71 in incident open fall rainwater; ii)
49 conductivity ranging from 21 to 166 $\mu\text{S}/\text{cm}$; and iii) dissolved organic carbon concentrations in
50 open fall and canopy throughfall of 16 ± 10 mg/L and 22 ± 12 mg/L, respectively; with incident
51 fluxes spanning 600 to 4200 mg C $\text{m}^{-2} \text{a}^{-1}$ across the transect. Ultimately, this demonstrates that
52 the customized precipitation sampling design of this new platform enables more universal
53 accessibility of deposition samples to the atmospheric observation community – for example, those
54 who have made community calls for targeting biogeochemical budgets and/or contaminants of
55 emerging concern in sensitive and remote regions.

56

57 **1.0 Introduction**

58 Atmospheric deposition is the central loss process for particles and gases to terrestrial and
59 aquatic surfaces (Pacyna, 2008). Particles and gases can be deposited by both dry and wet
60 deposition processes. Dry deposition is facilitated by the direct interaction of gases and particles
61 with boundary layer surfaces such as water, vegetation, and/or soil, while wet deposition involves
62 in-cloud scavenging and below-cloud interception of gases and aerosols by, e.g., rain droplets and
63 snow crystals (Fowler, 1980; Lovett and Kinsman, 1990). Dry and wet deposition are global
64 processes coupled to regional synoptic scale conditions, but their relative importance depends on
65 local sources and global transport of atmospheric analytes of interest. Dry deposition consists of a
66 variety of mechanisms for particles and gases, with fine mode particles and their chemical
67 constituents (compared to ultrafine and coarse mode particles) being more likely to undergo

68 atmospheric long-range transport prior to being deposited (Farmer et al., 2021). Wet deposition
69 occurs when such long-lived atmospheric particles and gases are included and/or scavenged into
70 cloud water and transported to the surface of the Earth in precipitation (e.g., snow and rain). With
71 the size and number of droplets in the atmosphere largely controlling the rate, wet deposition
72 depends on a variety of meteorological factors affecting precipitation, such as the size distribution
73 and concentration of ice and droplet nucleating particles, as well as the solubility, concentration,
74 and reactivity of gases (Lovett, 1994). Ultimately, deposition plays an important role in pollutant
75 distribution and biogeochemical cycling of long-studied major nutrients (e.g., nitrogen and sulfur
76 in acid rain) and those with increasing recognition of importance such as dissolved organic carbon
77 (DOC) (Meteorological Service of Canada, 2005; Vet et al., 2014; Safieddine and Heald, 2017;
78 United States Environmental Protection Agency, 2020).

79 Recognizing the significance of atmospheric trace chemical deposition has led to the
80 establishment of monitoring networks. For example, long-term wet deposition monitoring
81 networks, like the Canadian Air and Precipitation Monitoring Network (CAPMoN) and the
82 National Atmospheric Deposition Program (NADP), aim to provide critical data on the spatial and
83 temporal patterns of wet and dry deposition. As a result, this has allowed for the estimation of
84 regional and continental deposition rates of species regulated by national or international policies
85 (Lovett, 1994). Data from these networks have been critical to understanding the efficacy of policy
86 to reduce environmental issues like acid rain (Likens and Butler, 2020). In particular, the Oslo and
87 Geneva protocols have achieved an 80% decrease in both North American and European SO₂
88 emissions since 1980 (Grennfelt et al., 2020). Despite these successes, reduction in acid deposition
89 has had unexpectedly slow recovery in ecosystems leaving them sensitized – necessitating
90 continued deposition monitoring (Stoddard et al., 1999; Kuylenstierna et al., 2001).

91 Over the past 60 years, the precipitation chemistry community has made advancements in
92 deposition collectors to better understand atmospheric processes (Siksna, 1959). While bulk
93 deposition collection (i.e., a collection bucket or jug fitted with a funnel open at all times; Hall,
94 1985) is both a simple and economically feasible sampling method utilized by monitoring
95 networks, it is subject to bias through collection of inputs other than atmospheric deposition (e.g.,
96 bird droppings, insects, plant debris). As a result, bulk collectors can overestimate total deposition
97 and underestimate wet deposition in a variety of locations (Lindberg et al., 1986; Richter and
98 Lindberg, 1988; Stedman et al., 1990). Sequential precipitation collection methods include

99 manually segmenting samplers (requiring only a shelter, clean surface, and an operator), linked
100 collection vessels (sample containers that are filled in sequence via gravitational flow), amongst
101 others and have been developed to analyze rainwater composition and measure parameters such
102 as pH and conductivity (Gatz et al., 1971; Reddy et al., 1985; Vermette and Drake, 1987; Laquer,
103 1990). Sequential sampler designs have also been adapted to collect precipitation in remote field
104 sites (Germer et al., 2007; Sanei et al., 2010). Although it is a more costly and time intensive
105 method when compared to bulk deposition collection, the major appeal of measuring isolated wet
106 deposition is the ability to isolate this individual atmospheric process. Further innovation can
107 reduce bias and improve the preservation of samples, such as the use of sensors to automate
108 isolation of collected precipitation or the addition of polymeric mesh barriers to reduce debris input
109 in windy environments (Lovett, 1994) - yet commercial solutions often come at a substantial
110 expense.

111 When targeting biogeochemically relevant species in deposition collectors, additional
112 standard practices have been developed to improve the representativeness of sample composition.
113 First, an appropriate monitoring site must be selected. Three categories of siting criteria,
114 established by organizations such as CAPMoN and the NADP, are of particular importance: (i)
115 site representativeness and physical characteristics, (ii) distance from potential pollution sources,
116 and (iii) operational requirements (Canadian Air and Precipitation Monitoring Network, 1985a;
117 National Atmospheric Deposition Program, 2009). This means that each site must be a location
118 that receives precipitation representative of the hydrologic area; is ideally not within 500 m of
119 local pollution sources, such as wood-burning stoves, garbage dumps, and vehicle parking lots;
120 and is accessible for daily collections, maintenance, and can be serviced by reliable 115 volts of
121 alternating current (VAC) electrical power (Canadian Air and Precipitation Monitoring Network,
122 1985a; National Atmospheric Deposition Program, 2009). Despite these guidelines, there are many
123 reasonable scenarios in which these siting conditions cannot be met. As an example, remote sample
124 collections are often required for global assessments on persistent contaminants or nutrients of
125 biogeochemical importance. Remote locations, however, can result in sampling sites with no
126 power provision, infrequent sample collection, and/or the infrastructure-bearing location itself
127 being a source of the targeted pollutants. As a result, innovation in collection strategies such as
128 time-integrated off-grid sampling, with modularity in the deployment of replicates, as well as

129 materials for quantitative collection of environmental targets, is still needed to expand and/or
130 modify networks to meet current and future monitoring and policy needs.

131 In biogeochemical cycles, for example, improvement of constraints in atmospheric carbon
132 linkages to terrestrial and aquatic processes is necessary. This would play a critical role in correctly
133 assessing climate feedbacks and reducing uncertainty in Earth system models. The measurement
134 of atmospheric DOC transport to surfaces has been limited and impedes landscape scale carbon
135 balance from being obtained (Casas-Ruiz et al., 2023). The pool of compounds from which DOC
136 is derived in the atmosphere has also been limited and is only recently seeing an increase in
137 research intensity. Reactive organic carbon (ROC) is defined as the sum of nonmethane organic
138 gases and primary and secondary organic aerosols (Safieddine and Heald, 2017). The major
139 removal mechanism of water-soluble organic compounds produced through oxidation from the
140 atmosphere is by dry deposition of particle-bound pollutants and scavenging by rainfall (Jurado et
141 al., 2004, 2005). When ROC is scavenged into rainfall, it becomes DOC and enters terrestrial and
142 aquatic systems. Deposition measurements of ROC compounds are needed since they play a
143 crucial role in the formation of secondary species such as ozone, particulate matter, and carbon
144 dioxide (CO₂) (Safieddine and Heald, 2017; Heald and Kroll, 2020).

145 There are several evolving drivers around studying atmospheric ROC; for example, light-
146 absorbing organic carbon that can affect global radiative balance and undergo photochemical
147 transformations in the condensed phase (Saleh, 2020; Wang et al., 2021; Washenfelder et al., 2022;
148 George, 2023). Reactive organic carbon can also influence cloud formation and contribute to
149 precipitation acidity (Avery et al., 2006; Ramanathan and Carmichael, 2008). Measurements of
150 speciated ROC are difficult due to the chemical complexity of emitted compounds and oxidation
151 products (Heald and Kroll, 2020). To circumvent this, monitoring and quantifying DOC can be
152 used as a proxy to estimate the total ROC in precipitation. However, quantitative measurements of
153 DOC in precipitation samples are sparse due to its relatively low concentration of 0.1 to 10 mg C
154 L⁻¹ (Iavorivska et al., 2016; Safieddine and Heald, 2017). Recently, calls for carbon closure on
155 atmospheric processing of ROC make this measurement of increasing importance (Kroll et al.,
156 2011; Heald et al., 2020; Barber and Kroll, 2021). Similarly, to obtain net landscape or watershed
157 carbon exchange, studies require effective methods for capturing and preserving atmospheric DOC
158 deposition to constrain biogeochemical linkages at global interfaces as outlined above.

159 In this work, we present the design of a custom-built automated array of precipitation
160 samplers that can be operated both on- and off-grid for wet deposition collection. The purpose of
161 these samplers is to enable cost-effective collection of integrated water-soluble conductive
162 atmospheric constituents deposited in remote environments without grid power or routine access.
163 A sensor interfaces with a custom-built motor control board capable of operating up to six
164 independent wet deposition units such that canopy throughfall (TF) and incident precipitation
165 (open fall, OF) measurements are possible to collect in replicate. The materials used can be easily
166 changed in order to optimize collection and preservation of a wide array of target analytes, such
167 as DOC, when using high density polyethylene and mercuric chloride (HgCl_2). We demonstrate
168 that these platforms are capable of continuous operation off-grid for monthly wet deposition
169 collection of precipitation across the Newfoundland and Labrador Boreal Ecosystem Latitudinal
170 Transect (NL-BELT) during snow-free periods in 2015 and 2016. Extremes in system performance
171 were evaluated by testing the power consumption of a sampling array from spring through fall
172 when paired with a solar top-up system, and during snow-free winter conditions using only a
173 battery. The two years of field samples were collected using an array of six collection units, with
174 triplicate collection of both incident precipitation and throughfall from rain passing through a
175 forest canopy. Samples were analyzed in terms of deposition volumes relative to total bulk
176 volumes, reproducibility of replicate samples, and to determine the fraction of conductive rainfall
177 within the total volume of precipitation at these remote sites. The captured fraction compared to
178 total volume deposited is used to gain insight into how these samplers can limit analyte dilution
179 effects and improve method detection limits, such as rejecting 50% of the total volume delivered
180 as ultrapure precipitation leading to a factor of two improvement. Chemical parameters of pH,
181 conductivity, and DOC fluxes collected according to established preservation protocols were then
182 compared to prior measurements to validate this proof-of-concept system. Measurement methods
183 for pH and conductivity of rainwater are very well-established in the literature and serve as a
184 baseline reference to ensure that the samples collected by the new devices presented in this work
185 are consistent with what is expected in samples from a remote coastal environment, given the
186 selective sampling strategy. We then move away from these well-established parameters to
187 quantify DOC fluxes using established biogeochemical preservation techniques for fresh water
188 and groundwater to demonstrate the potential of these samplers in application to automated

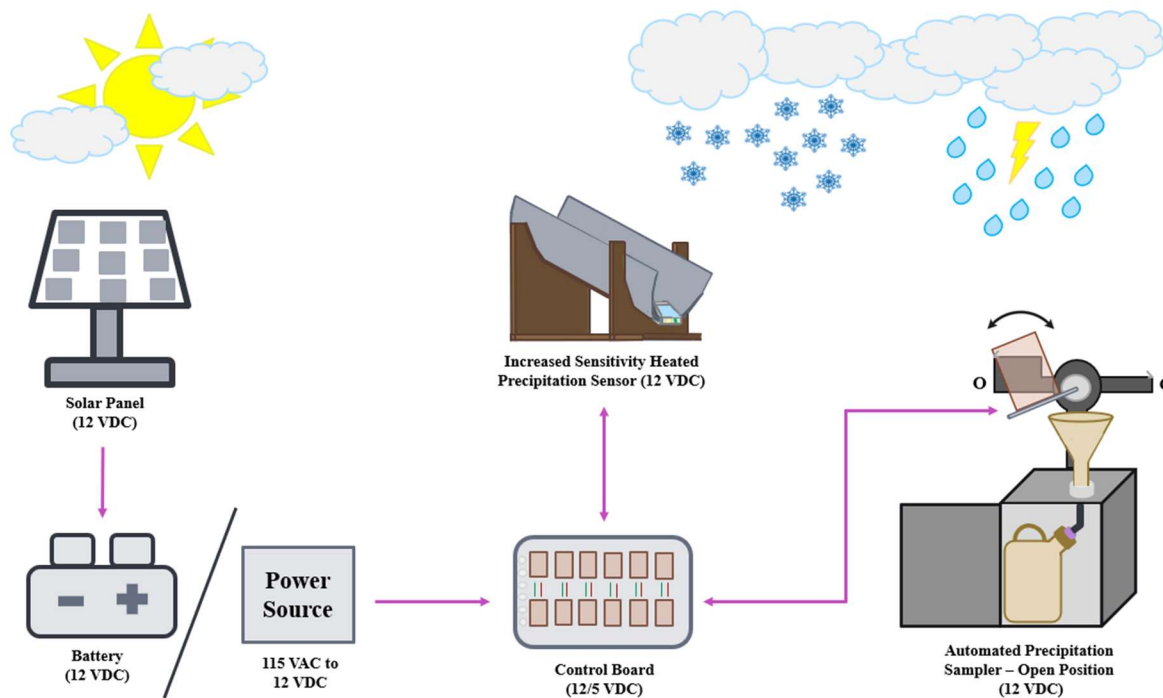
189 collection of analytes of emerging importance and interest in the remote locations of our latitudinal
190 transect.

191

192 **2.0 Materials and Methods**

193 **2.1 Precipitation Sampling Array Components**

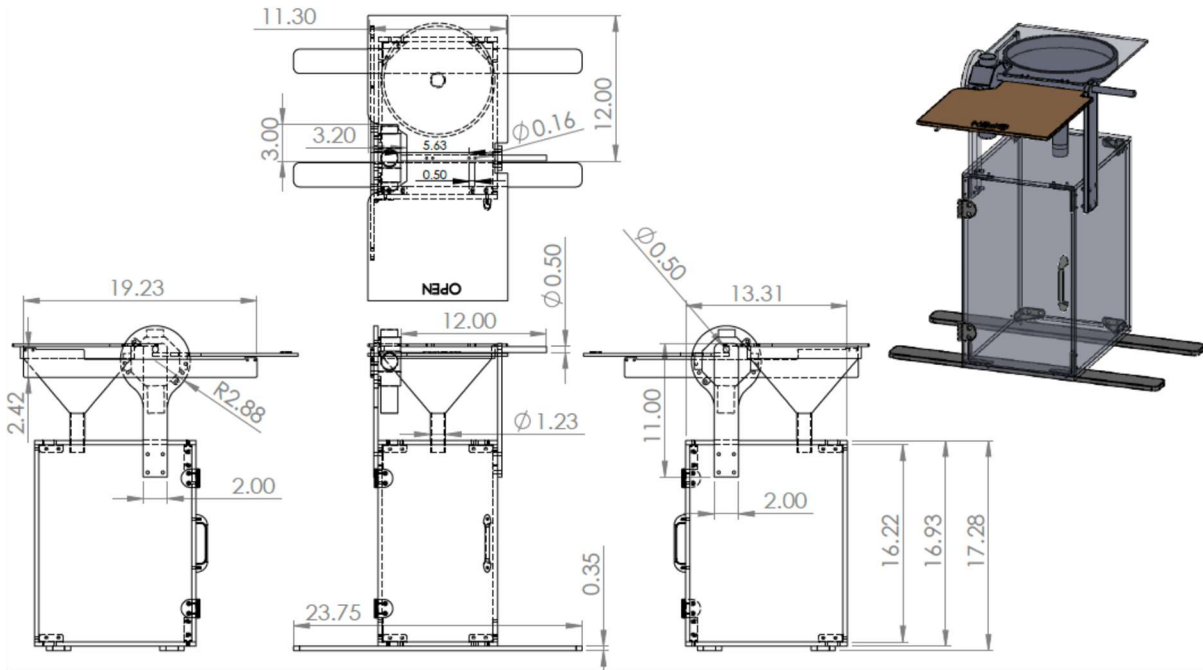
194 Each automated precipitation sampling setup can be operated as an array, here being used
195 in groups of up to six collection units (Figure 1). A collection unit is a simple opaque doored box.
196 The box protects the sample containers against exposure to direct sunlight and provides a mounting
197 location for the funnel and lid, while also facilitating easy exchange of sample containers. The
198 collection units can be fitted with stabilizing legs that allow them to be bolted to concrete or pinned
199 by retaining rods when on soil. In both cases, this prevents tipping and loss of sample during high
200 winds or wildlife-sampler interactions (e.g., Figures 2 and S1). The collection of precipitation is
201 facilitated by a funnel mounted through the top of the sampling unit. The funnel tip extends into
202 the opening of the sample collection container placed inside. The connection can be sealed to better
203 preserve volatile analytes with tubing that passes through a sealed grommet (P/N 9280K34,
204 McMaster-Carr) to enter the sample collection container and minimize evaporative losses.
205 Precipitation events are sampled selectively by modulating the position of a lid over the funnel
206 with an electric motor. The collection unit motors are operated by a digital control board, which
207 interfaces with a precipitation sensor and requires 12 volts of direct current (VDC) power supplied
208 to this system. Switches detecting the lid position ensure complete opening or closure of the funnel
209 mouth for each collection unit.



210
 211 **Figure 1.** Schematic of custom-built automated precipitation sampling array components for off-
 212 grid wet deposition collection. The pink arrows denote the direction of electrical signal and power
 213 exchanged between components. The curved black arrow indicates the rotation of a motorized lid
 214 to obtain open (O) or closed (C) sampler configurations.
 215

216 **2.1.1 Collection Units**

217 The collection unit materials to date have been made of both 3/8" plywood and black
 218 polyacrylate sheeting. The materials have demonstrated high durability on the order of four years
 219 under field conditions (Figures S1 and S2). Opaque materials were explicitly selected to minimize
 220 photochemical reactions and growth of photosynthetic microorganisms within the sample. The
 221 dimensions of the collection unit are detailed in Figure 2. Each can accommodate sample
 222 containers up to 20 L in volume for collection in locations with large monthly wet deposition
 223 volumes, such as in Newfoundland and Labrador (Table 1).
 224



225

226 **Figure 2.** Detailed collection unit schematic with all dimensions provided in inches. Further
 227 specifications for the lid dimensions can be found in Figure S3. The shaded 3D rendering depicts
 228 both open and closed states for the lid, positioning of legs to secure it to surfaces, placement of
 229 corner brackets, and the door handle and hinges.

230

231

232

233

234

235

236

237

238

239

240

241

242

243

244

245

The box panels can be joined using hardware inserts (P/N 1556A54 and 1088A31, McMaster-Carr, Aurora, OH), 3D printed corners (Figure S4), or along the box edges with screws if using wood. The door is attached with two hinges (P/N 1549A57, McMaster-Carr) and held closed with a magnetic contact (P/N1674A61; McMaster-Carr) or hooked latch. The electric motor controlling the lid is enclosed in a standard polyvinylchloride electrical junction box, which is attached to a short paddle mounted on one side of the collection unit. Here we used an electric worm-gear motor (12 VDC, 2 revolutions per minute; TS-32GZ370-1650; Tsiny Motor Industrial Co., Dong Guan, China) mounted inside the enclosure with matching hex bolts (P/N 91251A146, McMaster-Carr) that passed through the weather-tight cover while the drive shaft protrudes through a 3/8" hole drilled in the cover. The drive shaft has a flat edge to affix the lid rod using a short set screw (Figure S5) that is cemented semi-permanently in place with thread locking compound (P/N 91458A112; Loctite Threadlocker Blue 242; McMaster-Carr). The lid rod is 3/8" aluminum machined on one end to allow connection to the motor drive shaft (Figure S5) with four threaded holes along its length to affix the lid (Figure S3). The lid rod passes through a second mounting paddle on the box that keeps the lid level and capable of isolating the funnel from the

246 atmosphere in the absence of precipitation. The lids used here were made of 1/8" Lexan
247 polycarbonate sheet.

248 Selective precipitation sampling is performed using a logic-based assessment of sensor and
249 switch states (defined in Figure S6) by the control board quadNOR gate chip (Fairchild
250 Semiconductor P/N DM74LS02) which activates the H-bridge motor driver chipset (Figure S7).
251 A 12 VDC signal drives the clockwise or counterclockwise rotation of the motor, installed in a
252 suitable port of the junction box, via a cable from the control board, which passes through a
253 weather-tight compression fitting (e.g., Home Depot SKU# 1000116446). The motor rotation
254 signal is interrupted when the lid makes contact with one of two weather-tight limit switches (P/N
255 SW1257-ND; Omron, Digi-Key Electronics, Thief River Falls, MN) mounted on opposite ends of
256 a horizontal armature connected to the vertical motor mounting paddle (Figure 2). The switches
257 controlling the lid location ensure that the funnel is completely open or covered as necessary for
258 precipitation collection. The funnels used in this work are 20 cm in diameter and made from high-
259 density polyethylene (HDPE; Dynalon, P/N 71070-020, VWR International, Mississauga, ON). A
260 7" x 5" piece of filtration mesh (P/N 9265T49, McMaster-Carr) that was tied together as a fitted
261 cone insert with Nylon thread (e.g., fishing line) to prevent large debris entering the sampler
262 containers when used, for example, in the collection of TF precipitation under a forest canopy
263 when accompanying litterfall is also expected. The exit of the funnel directs the collected
264 precipitation into the narrow-mouth opening the container inside the collection unit, such as 20 L
265 HDPE jugs or 10 L HDPE jerricans (Bel-Art Products; P/N 11215-314, VWR International).

266

267 **2.1.2 Heated Precipitation Sensor**

268 The detection of rain modulates the opening and closing of the collection units by an
269 interdigitated resistive sensor (M152; Kemo Electronic GmbH, Geestland, Germany; Figures S6
270 to S8). This approach is consistent with established precipitation detection techniques used by
271 government monitoring programs (e.g., CAPMoN; Canadian Air and Precipitation Monitoring
272 Network, 1985a, 1985b). The rain sensor detects conductive deposition by the completion of a
273 conductive circuit when electrolytes bridge the connection between the interdigitated gold
274 electrodes. The sensor is supplied with 12 VDC from the power system to trigger a relay when
275 precipitation conductance above 1 M Ω ·cm conductivity is detected (determined experimentally,
276 see Section S1). This is equivalent to approximately 8 μ M sodium chloride. The sensor detection

277 limit reflects an upper limit of precipitation ion loading because the design of the rain chute leads
278 to an increase in surface area of more than a factor of 25 on which solutes can accumulate to
279 enhance the ionic content of the deposited water. An output of 12 VDC is sent to the digital control
280 board by the relay when rain is sensed, or 0 VDC in its absence, for signal processing and motor
281 control (Figure S7). When rain is sensed, the lid of each sampler in the array is simultaneously
282 opened (<5 seconds) and is dependent on the rotational rate of the lid motor. To increase the
283 sensitivity of this sensor and to extend the sampling duration when conductive atmospheric
284 constituents are completely washed out of the atmosphere, a sloped tin chute (e.g., Home Depot
285 SKU# 1001110514) was added to extend the surface of the rain sensor. The sensor was placed at
286 the end of the chute and sealed in place with caulking to allow water droplets to move easily from
287 the chute onto the sensor.

288 The angle of the chute can be adjusted to control the momentum of collected droplets so
289 that they collect on the sensor surface and only flow off it when the rate of precipitation exceeds
290 the sensor evaporation capability. When soil is available, two bent rods can be used to hold the
291 chute at the optimized angle of 10° (Figure S2). They are inserted into the soil and the chute is
292 affixed to the tops of the rods with zip ties passed through small holes drilled in the sides of the
293 chute, which are subsequently sealed with caulking. When soil is unavailable, for example in urban
294 environments, we have created a mounting frame to hold the chute at the optimized angle of 10°
295 (Figure S8). When precipitation is detected the sensor surface draws current up to 1.0 ampere (A)
296 into a heater to actively evaporate water from its surface so that it accurately detects the active
297 period of rain events. The heated sensor has undergone preliminary field tests and is also capable
298 of detecting ice and snow, provided they contain electrolytes.

299

300 **2.1.3 Power Supply Systems**

301 Power for this system can be supplied from a battery at 12 VDC or using a 115 VAC to 12
302 VDC transformer power supply (P/N 285-1818-ND; TDK-Lambda Americas, Digi-Key
303 Electronics). Depending on the duration of sampling and the time of year, the battery capacity can
304 be changed to suit power needs (Section 3.2.2). To provide sufficient power density in this study,
305 over one to two month-long collection periods, the battery capacity was carefully matched; with
306 top-up options implemented when prolonged or high-frequency precipitation was expected.
307 Absorbent glass mat (AGM) marine deep cycle batteries can withstand discharge events down to

308 less than 60 % capacity and are robust under nearly all environmentally relevant temperatures (\leq
309 -20°C to 40°C). Additionally, these batteries interface easily with solar charging options as they
310 are able to accept high current input. Monthly collections in Newfoundland were powered with 76
311 amp-hour (Ah) AGM batteries (Motomaster Nautilus; Ultra XD Group 24 High-Performance
312 AGM Deep Cycle Battery, 12 VDC) topped up by a 40 W solar panel interfaced with a charge
313 controller to prevent overcharging (Coleman; Model # 51840, max current of 8 A at 14 VDC).

314 For collections made every second month in Labrador, a 120 Ah battery with the same
315 solar top-up strategy was used to ensure continuous operation. For either remote field deployment,
316 batteries and charge controllers were housed in a Pelican™ case (Model 1440, Ocean Case Co.
317 Ltd., Enfield, NS) fitted with weathertight bulkhead cord grips (P/N 7529K655, McMaster-Carr)
318 through which charging and power cables were passed (Belden, Coleman; S/N 7004608,
319 70875227, Allied Electronics, Inc., Ottawa, ON). Humidity in all weatherproof cases was
320 minimized by exchanging reusable desiccant packs (Ocean Case Co. Ltd.) when depleted batteries
321 were exchanged for fully charged replacements. Solar panels were repositioned monthly to
322 optimize orientation for solar power provision. Using either power source, the control board
323 converts and distributes the 12 VDC to the other components in the precipitation sampling array.

324

325 **2.1.4 Custom Control Board**

326 A custom control board to operate a six-collection unit array was designed based on prior
327 digital logic circuits for standalone collectors (VandenBoer, 2009). The 12 VDC battery or
328 transformer output is supplied directly to the rain sensor and relay, as well as to the motor drivers
329 for lid opening (Figure S9). Each collection unit is controlled independently to ensure lids are fully
330 opened or closed, thereby requiring six replicate motor driver control circuits that respond to their
331 independent switch signals. The remainder of the signaling and digital logic operates on 5 VDC
332 which is produced by on-board voltage regulators (Micro Commercial Co; P/N MC7805CT-BP,
333 Digi-Key Electronics). The lid switches are provided with 0 and 5 VDC to indicate collection unit
334 open or closed status (Omron Electronics; P/N D2FW-G271M(D), Digi-Key Electronics). The
335 signals from the sensor and switches connect to the board through four-conductor cable (Belden;
336 S/N 70003678, Allied Electronics Inc.) passed through weathertight bulkhead cord grips and
337 secured to screw terminals (Figure S9). The sensor and switch signal inputs interface with a quad
338 NOR GATE chipset (Texas Instruments; P/N 296-33594-5-ND, Digi-Key Electronics) to trigger

339 the motor driver (STMicroelectronics; P/N 497-1395-5-ND, Digi-Key Electronics) such that it
340 rotates or remains stationary. The additional resistors, capacitors, and diodes are necessary to
341 maintain stable signaling throughout the printed circuit board (Figure S9, Table S1).

342 The custom control board was housed in a Pelican™ case (1400 NF; Pelican Zone,
343 Mississauga, ON) fitted with cut-to-use foam inserts and a reusable desiccant pack that was also
344 exchanged alongside those for the battery cases. All collection units, sensors, and power supply
345 cables were passed through eight weathertight bulkhead cord grips and fixed to screw terminals
346 on the board. The opposing ends of the cables were fitted with weathertight Bulgin Buccaneer 400
347 or 4000 Series circular cable connectors (Table S2; Allied Electronics, Inc.) to allow easy field
348 installation with mated connectors on the cables originating from each of the previously mentioned
349 array components. Connected cables could then be buried in shallow soil trenches to reduce the
350 attention of gnawing animals, as well as potential entanglement hazards with other wildlife.
351 Precipitation events were logged from the control boards using a HOBO 4-channel analog data
352 logger (UX120-006M; Onset®, Bourne, MA) that records the sensor, switch, and motor voltages.
353 The fourth channel is reserved to monitor battery or power supply voltages over time (Section 3.2).

354

355 **2.2 Power Demand and Management Tests**

356 Power demand was calculated based on the cumulative component requirements prior to
357 the selection of batteries. This was to ensure adequate capacity to collect samples over one to two
358 month-long field deployments and are sufficient for an assumed worst-case scenario of one week
359 of constant rain without solar power charge restoration. Solar panel power production capacity
360 was determined based on the calculated energy required to recharge the battery. As a result, we
361 selected the 40 W panel which could complete charging at 14 VDC with a week of direct sunlight
362 at 8 hours per day. The power demand for a six-sampler array was measured in standby and during
363 operation with a digital power meter (Nashone PM90, Dalang Town, China) in real-time when
364 supplying 12 VDC with a transformer. Contrasting power demand tests were performed under
365 different environmental conditions and power management configurations. The first was
366 performed using the 76 Ah AGM battery with a solar top-up in an urban environment from July
367 through August 2018, while the other was performed using a 103 Ah AGM battery alone from
368 January through February 2019. The dataset can be found in Colussi et al. (2024).

369

370 **2.3 Continuous Monthly Collection of Remote Samples at NL-BELT**

371 One array of six automated collection units (3 OF, 3 TF) were deployed within one forested
372 experimental field site located in each of the four watershed regions of the NL-BELT (24 samplers
373 in total) between 2015 and 2016. Additionally, between one to three total deposition samplers were
374 located at each of the four field sites (Table 1, Figure S10). The watersheds span 5.5° latitude from
375 the southernmost site Grand Codroy (GC), through the colocated Pynn’s Brook (PB) and Humber
376 River Camp 10 (HR) sites, to Salmon River (SR) as the highest latitude site on the island of
377 Newfoundland. The northernmost forested watershed, Eagle River (ER), is located in southern
378 Labrador and extensive details characterizing each of the four sites can be found in Ziegler et al.
379 (2017). All sampling locations are far from anthropogenic pollutant point sources, except for the
380 ubiquitous presence of marine sea spray from the nearby marine coastlines. The total deposition
381 samplers were identical to the automatic collection units except that they were not fitted with a
382 motor arm and lid, so they did not require a source of power. Three of the six automated samplers
383 were deployed in the open at a distance from the forest stand, equal to or greater than the height
384 of the trees, in line with CAPMoN and NADP guidelines. The other three automated samplers
385 were placed under the canopy to collect TF precipitation within the forest sites. These samplers
386 actively collected wet deposition into integrated monthly (Newfoundland) or two-month
387 (Labrador) samples during snow-free periods (approximately June through November). The arrays
388 were collected and stored during the winter months while total deposition samplers remained in
389 field locations year-round. It is also important to note that during the growing season, sample
390 collections were made at the same time – that is, OF and TF deposition were collected on a single
391 day at each sampling site and within a few days of each other across the transect. Collected sample
392 volumes were compared between the automated samplers and total deposition collectors for each
393 collection interval as a check on proper function (i.e., less than or equal volumes in automated
394 samples). During each site visit, the slope of the sensor was confirmed to be correct, sample
395 containers were collected and replaced with clean units, the battery and desiccant packs replaced
396 with fully recharged devices, and the entire array confirmed operational.

397

398

399

400

401 **Table 1.** NL-BELT sampling site details provide locations and identifiers, alongside those from
 402 long-term weather stations operated by Environment and Climate Change Canada (ECCC). Soil
 403 pH was determined from samples collected at the same time as precipitation. Mean annual
 404 temperature was derived from ECCC climate normals. Annual total deposition precipitation
 405 volumes were either measured for the 2015-16 period (ECCC, This Work) or calculated by the
 406 Oak Ridge National Lab DAYMET archive.
 407

Sampling Site	Sampling Site Location	Station (Climate ID)	Station Location	Soil pH ^a	MAT (°C) ^b	Average Annual Precipitation (L)		
						ECCC ^c	DAYMET ^g	This Work
Grand Codroy (GC)	47°50'43.1"N 59°16'16.0"W	Stephenville A (8403801)	48°32'29.00" N 58°33'00" W	3 to 4	5.0 ^e	53.2	58.9	45.6 (+5.17)
Pynn's Brook (PB)	49° 05' 13.20"N 57° 32' 27.60" W	South Brook Pasadena (8403693)	49°01'00" N 57°37'00" W	3 to 4	4.6 ^e	21.4	54.3	38.6 ^h
Salmon River (SR)	51°15'21.6"N 56°08'16.8"W	Plum Point (40KE88)	51°04'00" N 56°53'00" W	3 to 4	2.4 ^e	47.1	45.4	32.3
Eagle River (ER)	53°33'00.0"N 56°59'13.2"W	Cartwright A (8501100)	53°42'30" N 57°02'06" W	3 to 4	0 ^d	- ^f	56.3	25.8

408
 409 ^aSoil pH for the organic and mineral soil horizons determined by addition of 400 µL of aqueous 0.5 M CaCl₂ to a 50:50 w/w slurry
 410 of dried soil in deionised water. Note: the four remote NL-BELT sites are dominated by balsam fir trees underlain by humo-ferric
 411 podzol soil with pH ranging between 3.0 and 4.5.
 412 ^bEnvironment Canada: Canadian Climate Normals, 1981 to 2010, https://climate.weather.gc.ca/climate_normals/ (last accessed:
 413 14 July 2023).
 414 ^cAt least 20 years of measurements.
 415 ^dThe World Meteorological Organization's "3 and 5 rule" (i.e., no more than 3 consecutive and no more than 5 total missing for
 416 either temperature or precipitation).
 417 ^eAnnual precipitation averages determined using ECCC daily precipitation reports.
 418 ^fLarge quantity of missing data for this location from January 2015 to December 2016 prevents any reliable estimate.
 419 ^gEstimated deposition rates converted to volume using DAYMET (Thornton et al., 1997, 2021, 2022).
 420 ^hVolumes merged for 2015 and 2016 at PB and HR.
 421
 422

423 2.3.1 Sample Preservation

424 Four of the six sample containers (two each of OF and TF) were biologically sterilized
 425 using 1 mL of a saturated aqueous solution of mercuric chloride (HgCl₂) to preserve against
 426 biological growth and loss of bioavailable nutrients over the collection periods. Unsterilized
 427 sample containers (without HgCl₂) were used for measurements of recalcitrant species and to
 428 assess any matrix effects exerted on target analyte quantitation. The use of HgCl₂ as a sample
 429 preservation technique has been long-studied and well-established (Kirkwood, 1992; Kattner,
 430 1999); thus, additional tests to verify the preservation of collected chemical species over time were

431 not performed. The analysis of deposition collected in unsterilized and sterilized containers,
432 however, serves as a method for internal sample validation - as does our evaluation of measurement
433 outcomes in comparison to those reported within the literature. Collected sample volumes were
434 measured with a 1000 ± 10 mL graduated cylinder and aliquots were collected for chemical
435 analysis via transfer to precleaned 500- or 1000-mL HDPE containers (Nalgene; VWR
436 International). Samples were stored at 4°C before returning to the laboratory where they were
437 filtered with a 1000 mL Nalgene vacuum filtration system (P/N ZA-06730-53; ThermoFisher
438 Scientific, Waltham, MA), fitted with $0.45\ \mu\text{m}$ polyethersulfone filters (PES, P/N HPWP 04700,
439 EMD Millipore), to remove suspended solids. Filtered samples were transferred to new clean
440 HDPE containers and stored for up to two months at 4°C in a cold room until analysis. The target
441 analytes in this work are non-volatile and the described sample collection methods consider this
442 analyte property, as well as their interactions with container materials. The versatility of the system
443 design allows for the use of different collection materials, keeper solvents for volatile organics,
444 etc., so that the experimental design can be analyte specific, depending on end user needs. Sample
445 preservation approaches should thus be identified by users of this new platform based on their
446 scientific objectives and review of the literature (Galloway and Likens, 1978; Peden et al., 1986;
447 Dossett and Bowersox, 1999; Wetherbee et al., 2010). In addition to the internal validation
448 approach described here, we aim to demonstrate that the precipitation samplers in this work are
449 suitable for measuring conductive deposition on- and off-grid. Below we highlight autonomous
450 off-grid operations, determine the fraction of conductive rainfall collected from the total volume
451 of precipitation, and validate our measurements through comparison to the literature.

452

453 2.4 Cleaning and Preparation of Sample Containers

454 All sample collection and storage containers, as well as all sample handling apparatuses,
455 were made of HDPE or polypropylene for the quantitative analysis of target analytes. Prior to use
456 in handling samples, these were all acid-washed in 10 % v/v HCl (P/N BDH7417-1; VWR
457 International) followed by six sequential rinses with distilled water and ten rinses with 18.2
458 $\text{M}\Omega\cdot\text{cm}$ deionised water (DIW; EMD Millipore Corporation, Billerica, MA, USA). Containers
459 were dried by inversion on a clean benchtop protector overnight, or with protection from dust using
460 lint-free lab wipes over container openings when necessary. Field and method blanks were
461 collected through the addition of DIW to cleaned containers, and/or sample handling devices, in

462 order to quantify appropriate method detection limits and to identify any sources of systematic or
463 random contamination. Blank subtraction was applied to measurements, where appropriate.

464

465 **2.5 Measurements of pH and Conductivity**

466 The pH and conductivity of each sample was determined using a ThermoScientific™ Orion
467 Versa Star meter (ORIVSTAR52) interfaced with a pH electrode (Model: 8157BNUMD, Ultra
468 pH/ATC Triode, ROSS) and 4-electrode conductivity cell (Model: 013005MD, DuraProbe,
469 ROSS). Prior to use, the probes were calibrated daily with standard solutions specific for these
470 probes (ThermoScientific™ Orion™ conductivity standard 1413, and pH 4, 7, and 10 buffers) and
471 then stored between analyses according to manufacturer directions. Aliquots of 15 mL of
472 precipitation from archived samples were subsampled into 40 mL polypropylene Falcon tubes.
473 This was followed by immersion of a cleaned electrode for the conductivity measurement,
474 followed by the pH probe measurement to prevent conductivity bias due to potassium chloride
475 migration across the glass frit of the pH probe. Readings were recorded once signals had stabilized.

476 **The datasets can be found in Colussi et al. (2024).**

477

478 **2.6 Measurements of Dissolved Organic Carbon (DOC)**

479 Measurements of DOC were performed by catalytic combustion of samples in a platinum
480 bead-packed quartz furnace at 720°C to quantitatively produce CO₂, followed by non-dispersive
481 infrared absorption spectrophotometry using a Shimadzu Total Organic Carbon (model: TOC-V)
482 analyzer and an autosampler (model: ASI-V). Cleaning of materials prior to DOC determination
483 follows the same procedure as for the sample containers. Precipitation aliquots of at least 12 mL
484 were transferred to clean and combusted (500°C, 5 hours) 40 mL borosilicate glass vials, then
485 capped and stored at 4°C until analysis. Prior to analysis, vial caps were replaced with cleaned
486 polytetrafluoroethylene-lined septa. Inorganic dissolved carbon (e.g., H₂CO₃) was purged from
487 samples by acidification to pH 2 with HPLC grade H₃PO₄ (20 % v/v) and bubbling with an inert
488 carrier gas. Samples were analyzed in triplicate and quantified using calibrations spanning 0.1 to
489 10 or 10 to 100 ppm (mg C L⁻¹) with potassium hydrogen phthalate (KHP), depending on the
490 relative sample concentration range. Accuracy and precision were assessed using 1 and 10 ppm
491 KHP check standards analyzed every 10 injections, respectively. Calibrations were performed at
492 the beginning of every analysis day. **The dataset can be found in Colussi et al. (2024).**

493 **3.0 Results and Discussion**

494 In addition to the general design advantages in the section that follows, we present the
495 results of various physical and chemical parameters to validate this new open source custom-built
496 modular system. The power consumption and snow-free performance testing are used to
497 demonstrate the off-grid capabilities of these samplers, as are the two-year datasets. The lower
498 power requirements are compared to existing commercial samplers and paired with solar top-up
499 to prolong the use and reduce the need to replace batteries on timescales shorter than planned
500 sampling duration (i.e., < 1 month). We then evaluate the automated wet deposition volumes, in
501 which the samplers prevent dilution during atmospheric washout events, compared to total
502 volumes collected from co-located samplers to depict the fractionation by volume as a function of
503 time. We also investigate the advantages of replicates collected across the four watersheds, using
504 deployments of triplicate samplers under field conditions. The ratio of collected TF to OF
505 replicates highlights the ability of these samplers to capture the dynamic nature of precipitation
506 interacting with forest canopies. Simple pH and conductivity measurements are then used as
507 benchmarks to situate the NL-BELT data within the established literature to emphasize the robust
508 operation of the samplers and impact of the selective sampling. Fluxes of DOC are also
509 interrogated across all four sampling sites as we demonstrate the potential of these samplers to
510 make measurements of more complex analyte pools that are of current interest to the atmospheric
511 measurement community.

512

513 **3.1 General Design Advantages**

514 While several precipitation collectors have been similarly developed to address specific
515 scientific objectives – e.g., the quantitation of dust in wet and dry deposition (Laurent et al., 2015;
516 Brahney et al., 2020), determination of ions and DOC in a tropical rainforest (Germer et al., 2007)
517 and urban environments (Audoux et al., 2023), here we present a more general design for modular
518 adaptability. When compared to other precipitation collection apparatuses, the automated
519 precipitation sampler developed in this work has several advantages. Most notable is the ability to
520 collect integrated samples at remote locations by exploiting its off-grid capabilities. Our approach
521 also maximizes the sensitivity of the rain sensor as long as electrolytes remain in the water reaching
522 it. The chute ensures that even if the precipitation contains ultra-trace analyte quantities, they are
523 still collected and quantified for an extended period when high-purity water may be deposited

524 during an atmospheric wash-out event. The chute does this by accumulating water-soluble
525 materials between rain events that require time to be completely washed off and through the release
526 of ions from the material itself, which ages under environmental conditions. As the conductivity
527 of the precipitation falls below the sensor threshold – conductive precipitation being that which
528 initially contains high solute levels that progress through trace level concentrations, the added ions
529 from the chute prolong the collection of rain past this time point. In rainfall events where extended
530 atmospheric wash-out occurs, where precipitation becomes ultrapure water, the sampler lids will
531 eventually close – preventing dilution of the sample while maintaining the collection of analytes
532 of interest. A recent study has found that rainfall events could exhibit variability and the lower
533 atmosphere can be supplied with aerosols due to specific sources, atmospheric dynamics, and
534 meteorological conditions (Audoux et al., 2023). If this occurs, the automated lid will reopen to
535 sample the polluted air masses. In application to trace pollutants, this also reduces methodological
536 sample preparation time as it decreases the extent to which additional handling steps, like solid-
537 phase extraction, are required prior to analytical determinations.

538 The six replicate measurements used in each array provide a means of assessing sampling
539 reproducibility (e.g., canopy TF has expected heterogeneity) and for multiple analyte classes to be
540 targeted. Various analytes, with different chemical properties and/or contamination considerations,
541 can be targeted by changing the materials used for the components that encounter the sample (i.e.,
542 lids, funnels, and sample holding containers). Replicate collection can also allow for selective
543 sample preservation when quantifying deposited chemical species that may be reactive, volatile,
544 or biologically transformed. The modularity of the overall system design also allows the collection
545 units to be dismantled entirely and easily reassembled on-site, minimizing logistical issues and
546 costs for transport to remote regions. Lastly, these collection units are cost-effective. We were able
547 to produce four arrays, each consisting of six collection units, at a fraction of the cost of a single
548 equivalent commercial off-grid automated precipitation sampling unit.

549 With the majority of commercial precipitation samplers requiring a source of electricity,
550 on-grid sample collection necessitates high infrastructure costs and/or samplers being positioned
551 closer than desired to point sources of anthropogenic pollution. As a result, especially in remote
552 locations, site selection becomes heavily restricted and expensive when factoring in all the
553 standard criteria, particularly with respect to the need for an easily accessible power source. Thus,
554 the off-grid capabilities of our samplers lend dexterity to these systems and makes deposition

555 sampling that follows standard siting guidelines, like those of CAPMoN or NADP but without
556 power, more accessible to the global atmospheric research community (Vet et al., 2014). To further
557 highlight and validate their capabilities, a series of fundamental performance parameters were
558 collected and are discussed in detail in the sections that follow.

559

560 **3.2 Power Consumption and Performance Testing**

561 **3.2.1 Power Consumption of Instrumental Setup**

562 The simplicity of the automated precipitation samplers allows for low power consumption
563 during operation, which is particularly important for off-grid operation. The motors operating and
564 rain sensor heating during active precipitation are the most energy-intensive elements of the system
565 (Table 2). The integrated contribution of the motor over a month-long sampling period is however
566 negligible compared to other components, since it is operational for short periods of 5 to 10
567 seconds with a current usage of only 38 mA. The continuous need to provide 5 VDC to the digital
568 logic via step-down from 12 VDC is actually the largest power consuming component of the setup
569 in the absence of rain. When the samplers are in the closed position, under rain-free conditions,
570 the power consumption of the entire array is 4.66 Watts (W) and 2.86 W for transformed 115 VAC
571 and battery 12 VDC supplies, respectively. The provision of 12 VDC to the board with a
572 transformer for the 115 VAC application results in greater total power requirements. These values
573 increase to 10.00 W and 5.04 W with the detection of a conductive liquid on the precipitation
574 sensor as it heats the sensor surface to capture the active period of the event. Based on the measured
575 power consumption, a fully charged 103 Ah AGM battery would provide at most 447 hours (or 18
576 days) in standby mode under rain free conditions and 294 hours (or 12 days) if the heated surface
577 of the sensor is in continuous use (Table 2). The lower range limit is unlikely since the sensor only
578 operates for the duration of a rain event, after which the battery is available for solar top-up again.
579 In the fieldwork conducted here, battery life was extended through the addition of 40 W solar
580 panels to the systems. The entire array was confirmed to be operational at the end of monthly (SR,
581 PB, and GC) and two month (ER) integrated sampling periods on an ongoing basis, prior to
582 exchange with a new fully charged battery, for two years.

583

584

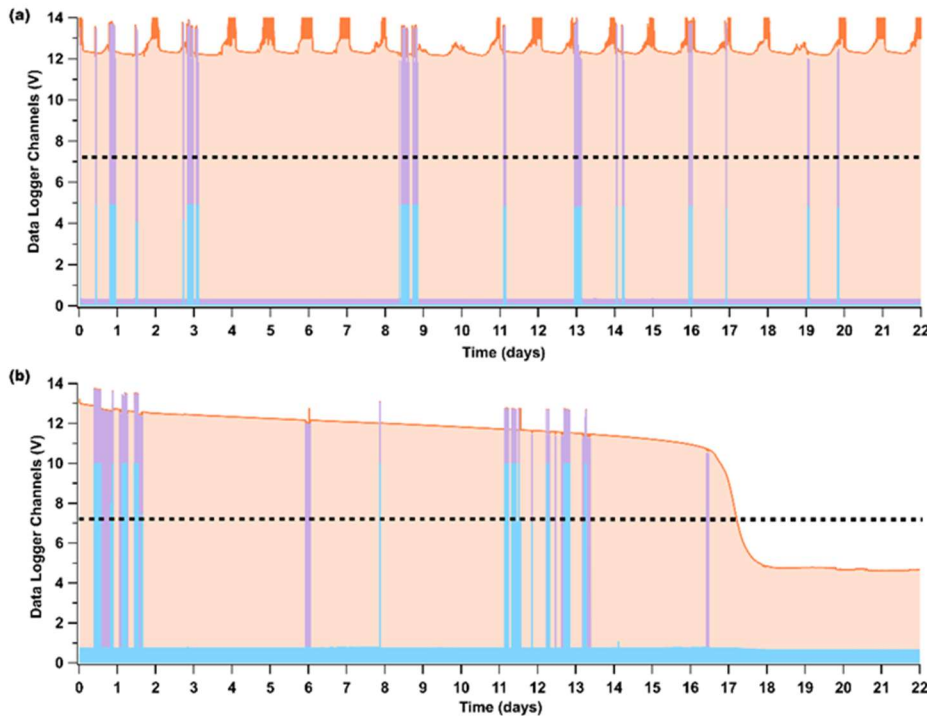
585 **Table 2.** Measured voltage, current, and power consumption of the rain sensor and circuitry in
 586 both the idle and maximally operational state when connected to a 12 VDC battery or transformed
 587 115 VAC. Total power demand was measured for wet and dry sensor scenarios.

Parameters	Rain Sensor		AC Outlet		DC Battery		Total			
	Idle	Active	Idle	Motors	Idle	Motors	AC Outlet		DC Battery	
			Board	In-Use	Board	in-Use	Dry	Wet	Dry	Wet
Voltage (V)	12 DC	12 DC	114 AC	110 AC	12 DC	12 DC	-	-	-	-
Current (A)	0.008	0.120	0.040	0.078	0.230	0.300	-	-	-	-
Power (W)	0.10	1.44	4.56	8.58	2.76	3.60	4.66	10.00	2.86	5.04

588
 589 In comparison to two commercial samplers used by national monitoring networks, the
 590 power requirements of our new samplers are substantially lower. The first commercial sampler we
 591 reviewed draws a maximum of 2 A, with a ceramic heater housed within the sampler case that
 592 draws 0.8 A constantly, resulting in an upper limit power demand of 230 W (at 115 VAC) and a
 593 lower limit of 92 W. The commercial sampler can be upgraded to utilize a thermostated space
 594 heater for winter operation, drawing an additional 4.2 A (480 W), resulting in a maximum power
 595 demand of about 800 W when using a 115 VAC power supply. A second commercial precipitation
 596 sampler reviewed is used by national monitoring networks and draws approximately 5 A, resulting
 597 in a power requirement of 575 W at 115 VAC. The commercial and standard precipitation samplers
 598 for deposition monitoring programs have much higher power requirements compared to those
 599 presented in this work. The commercial samplers utilize 80 to 100 times more power. With our
 600 lower power requirements, the new automated samplers prove to be advantageous in both on- and
 601 off-grid sampling yet are disadvantaged in being unable to collect snow in the winter.

602
 603 **3.2.2 Precipitation Sampler Performance Tests and Data Logging**

604 In addition to low power consumption during precipitation sampling, a supplied battery
 605 can obtain constant power renewal when outfitted with a solar top-up that is kept exposed to
 606 sunlight by proper orientation. At NL-BELT, adjustments were made for this during each site
 607 visit during sample collection. During the solar top-up tests below, voltages of the sensor and
 608 batteries were consistently monitored. Over a test period of 22 days, no appreciable decline in
 609 battery performance of a 76 Ah unit was observed despite the detection of more than 10 rain
 610 events during that period (Figure 3a).



612

613 **Figure 3.** Performance of off-grid precipitation samplers during sample collections from (a) 13
 614 July to 7 August 2018, using a 76 Ah battery and solar panel top-up and (b) 22 January to 13
 615 February 2019 with a 103 Ah battery and no solar panel. Battery voltage (shaded orange) is
 616 elevated above 12 VDC when charging, or decreases over time when no solar panel is used and
 617 precipitation is sensed/collected. The 12 VDC rain sensor relay signal (purple) and the open
 618 sampling lid switch voltage (blue) indicate active periods of detected precipitation. The black
 619 dashed line indicates the 60% efficiency cut off, 7.2 V, at which the battery should be recharged.
 620

621 In comparison, winter sampling with these devices is not recommended without substantial
 622 investment in a sufficient power density provided high-performance cold weather batteries. The
 623 lack of sunlight during winter at higher latitudes also negates the use of effective small scale solar
 624 top-up. Our tests show that when the samplers were deployed without a solar backup under snow-
 625 free winter conditions (temperatures ranging from -17.8 to 7°C), with a 103 Ah battery, the off-
 626 grid system only lasted for 17 days. At this point, the larger capacity battery was fully depleted by
 627 frequent snow and rainfall – probably due to the heated precipitation sensor requiring additional
 628 energy to phase change snow and ice to water and then to evaporate that water. This depletion
 629 occurred despite housing the battery in an insulated enclosure during the test. In addition, on days
 630 6 and 16, the precipitation sensor relay was activated but the lid did not rotate to the open position
 631 (Figure 3b, blue trace). This could have been because the precipitation event was not intense

632 enough for the lid to open fully and trigger the 5 V lid open switch or because of snow and ice
633 buildup around the lids resulting in them being unable to physically open. Overall, these samplers
634 may be possible to deploy during the winter if line power can be supplied. Such a deployment
635 would further necessitate that the sampling funnel be heated to render a liquid sample for collection
636 in the jugs in addition to the sensor chute to prevent snow and ice accumulation. A heated funnel
637 would also prevent snow or ice accumulation on top of the automated lids. Together, such power-
638 hungry requirements for winter operation exceed simple off-grid use with a battery package that
639 is easily transported into and out of remote field sites.

640

641 **3.3 Comparison of Sample Collection Volumes**

642 The automated samplers were colocated with total deposition samplers and deployed across
643 the experimental forests of four NL-BELT regions during the 2015 and 2016 growing seasons to
644 observe deposition trends. In addition, we compare these observations to the long-term climate
645 normals reported by ECCC and estimated deposition at 1 km x 1 km resolution from the DAYMET
646 reanalysis model (Table 1, Section S2). Three automated samplers were deployed in the open to
647 collect incident precipitation (OF) and another three under the experimental forest site canopy
648 (TF). The mean OF volumes of triplicate measurements from south to north were 1.42, 1.38, 1.31,
649 and 0.79 L, whereas the corresponding TF volumes were generally similar in magnitude at 0.96,
650 0.98, 1.02, and 1.13 L, for the 2015-16 sampling period (Figure 4). It is evident that the volume of
651 precipitation decreased as latitude increased for OF samples, whereas the opposite relationship
652 was observed in TF samplers, although the absolute volumes are more comparable in magnitude.
653 The total deposition volumes collected were as expected, decreasing from south to north in
654 agreement with the expectations from the long-term normals and comparable to the estimates from
655 the DAYMET model (Table 1), where the largest integrated volume of precipitation was collected
656 at the lowest latitude (GC) and a lower amount at the highest latitude (ER), with the intermediate
657 sites (HR and PB) having the lowest inputs overall during this observation period. Total annual
658 deposition volumes collected by our deployed samplers from south to north in 2015 were 39.5,
659 39.4, 31.9, and 17.5 L, while in 2016 they were 51.7, 37.8, 32.8, and 34.2 L. Total deposition
660 volume collected from HR was used for comparison to automated sample volumes collected at PB
661 in 2015, as they both share the same watershed. This approach had to be taken, as the HR site was
662 initially planned for full experimental use before becoming inaccessible in early 2015. The relative

663 error between the two sites for samples collected in 2016 was $\pm 15\%$ (24.6 L in PB and 32.2 L in
664 HR), comparable to the reproducibility we observe for replicates collected within a given site (see
665 below). The total deposition samplers were installed in HR in late 2014 and the automated samplers
666 were then set up at PB. Despite this, there is good agreement between the trends in predicted
667 deposition values by DAYMET with the measured values, although the absolute amounts from
668 these are systematically lower in all of our observations (Section S2). Regardless, by following the
669 recommended siting criteria from the NADP and CAPMoN as best as possible, the very strong
670 agreement of our temporal trends at both annual and monthly timescales with both comparators
671 demonstrates the suitability of the total deposition samplers and, therefore, the automated samplers
672 for use in quantifying deposited chemical species of atmospheric interest into the experimental
673 sites.

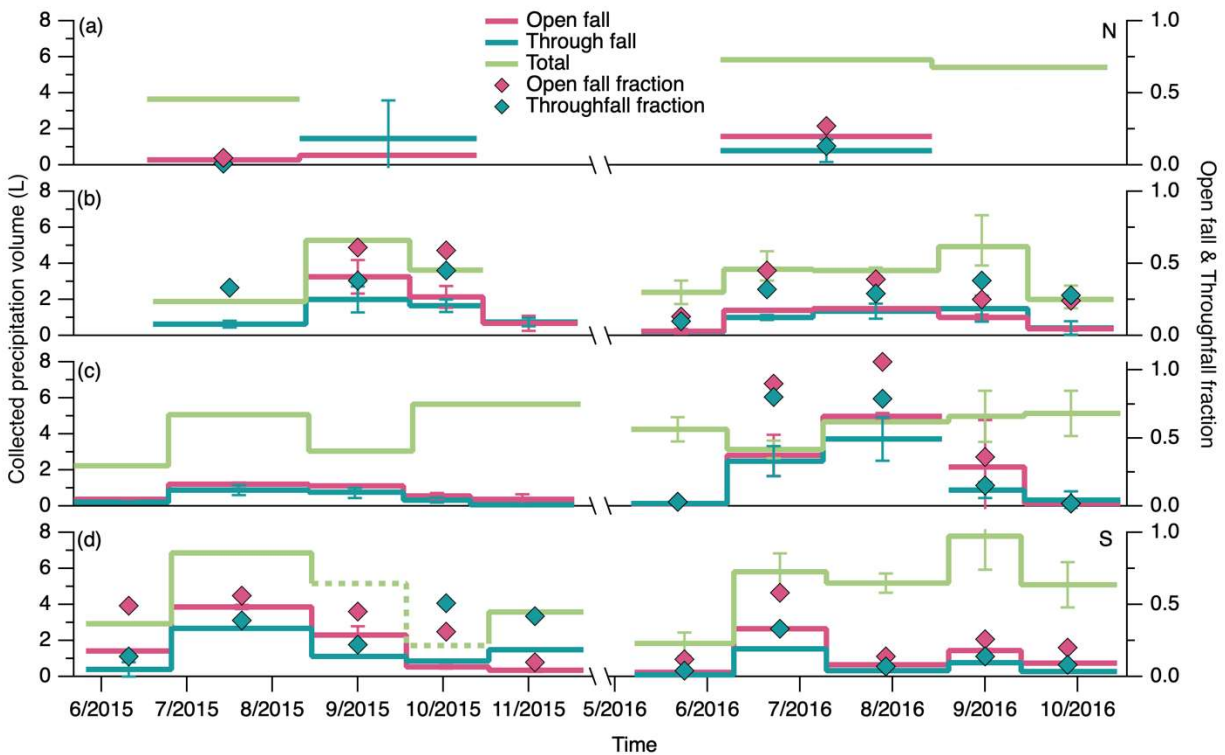
674 The wet deposition volumes collected for the snow free period using the automated
675 precipitation samplers did not follow the trends in total deposition (Figure 4), as might be expected
676 (e.g., due to pollutant loading, rainfall quantity/rate, and scavenging processes). For the 2015
677 collection period from June through October, the summed volumes of OF precipitation, from south
678 to north across the NL-BELT, were 25.4, 10.9, 20.4, and 2.2 L, while in 2016 they were 17.3, 30.4,
679 13.5, and 5.1 L. While the total and OF fractions would typically be much closer to unity in more
680 polluted regions, it would be expected in these remote NL-BELT field sites for the differences to
681 be driven by complex, non-linear processes that cannot be easily disentangled. Here we present
682 three reasons as to why the measured wet OF deposition volumes do not follow the total deposition
683 trend across the transect. First, these samplers are designed specifically to collect only conductive
684 precipitation (i.e., containing conductive atmospheric compounds) not total/bulk precipitation. As
685 a result, the OF wet deposition volume collected across the sites is mostly below 50% of total
686 volumes collected, while TF volumes are similar in magnitude or lower than that of OF (Figure
687 4). The wet deposition fraction collected was variable within and between regions, sometimes less
688 than 10%, despite large volumes collected in total and presumably due to intense atmospheric
689 washout that this region is well-known for. Second, the NL-BELT total deposition trend estimated
690 using the ECCC long-term climate normals represents a 30-year period (Bowering et al., 2022)
691 while the automated volume measurements here represent two years of targeted conductive
692 precipitation collection. The combined summed volumes of targeted conductive wet deposition
693 across the 2015 and 2016 field seasons were 42.7, 41.3, 33.9, and 7.3 L, somewhat better reflect

694 the expected precipitation trends within the transect (Table 1). Lastly, our monthly automated wet
695 deposition sample collection periods occurred from June through November and so it is temporally
696 incomplete with respect to the substantial amount of precipitation volume deposited as snow
697 delivered during the winter (Table S3). The discrepancies between the long-term trends and our
698 shorter-term observations therefore make sense as they are sensitive to interannual changes in
699 synoptic scale transport and rainwater solute loadings, as exemplified by the volumes collected in
700 SR in 2015 (Figure 4b) and PB in 2016 (Figure 4c). Overall, for the automated sampler
701 observations on a per-year basis, there is no consistent trend between site latitude and the volume
702 collected in either OF or TF. This is unsurprising as they are dependent on the conditions that drive
703 the rate of atmospheric wash-out and presence of conductive solutes.

704 The automated OF wet deposition volumes collected each year have peak values that range
705 from 1 to 4 L with an overall variability of $\pm 33\%$ for any triplicate of samples across the entire
706 dataset. Across our 33 sample collection periods, our replicate relative standard deviations (RSDs)
707 follow a log-normal distribution where volume reproducibility is typically within $\pm 12.5\%$ and
708 almost always within $\pm 31.5\%$ (Figure S11). A few outliers with higher variability skew the overall
709 view of volume precision. Out of 33 OF samples collected, 10 have RSDs greater than 40.5% with
710 2 of those 10 having RSDs greater than 100%. Those values greater than 40.5% had no systematic
711 relationship with site or time of time. Wind speeds were considered as a possible source of
712 variability. The prevailing winds over Atlantic Canada are known to be southwesterly in the
713 summer – intensifying during the autumn months – and westerly to northwesterly in the winter
714 (Bowyer, 1995; Jacob, 1999; Randall, 2015). Strong wind speeds (i.e., >100 km/hr) could occur
715 on an event basis during any time of the year and, thus, could contribute to the variability seen at
716 each field site. Wind is known to generate bias in gauge-based precipitation measurements where
717 unshielded precipitation gauges can catch less than half of the amount of a shielded gauge (Colli
718 et al., 2016). A windscreen design for obtaining rainfall rates – and thus, volumes – to be more
719 reproducible could be considered in future deployments of our developed samplers, similar to
720 recently reported innovations for smaller rainfall rate devices (Kochendorfer et al., 2023). This
721 would, however, increase costs and logistical considerations in deploying the developed devices
722 which currently operate synonymously to deposition systems employed by government monitoring
723 programs. Our siting approach is consistent with these, which often deploy a single sampler
724 without wind protection. Thus, by employing replicates, we are able to ascertain the environmental

725 variability. In addition, collection of replicate samples allows our observations to span a wider
726 physical area, reducing the impact of confounding variables such as wind speed in comparison to
727 a more typical sample size of one for many field collections. Imperfect siting and lack of shielding
728 is necessary where remote field sampling prevents the setup of such infrastructure. As a result, the
729 deployment of triplicate samplers provides researchers with a better opportunity to implement
730 quality control as they can reduce bias in the event of dynamic OF. While the effect of wind is
731 reduced, additional factors can drive variability when the samplers are placed under a forest canopy
732 for TF collection.

733 To demonstrate canopy dynamics impacting interception volumes within the sampling
734 sites, the ratio of throughfall to open fall (TF/OF) volume was compared amongst our total pool
735 of 31 samples. This group of samples encompassed the monthly average TF/OF values for each
736 set of triplicate samplers, at all four sites, from 2015 to 2016. These measurements were then split
737 into two separate populations – samples that have a TF/OF less than one ($n=24$) and those that
738 have a TF/OF greater than one ($n=7$). The samplers were positioned identically between years and
739 no single sampler was reproducibly found in the second population. In the first population, the
740 fraction collected was $56 \pm 21\%$ (ranging from 19 to 88%), likely due to the known processes of
741 canopy and stem interception (Eaton et al., 1973; Howard et al., 2022). For example, in two young
742 balsam fir-white birch mixed forest stands, the amount of precipitation intercepted by the forest
743 canopy, in similar snow-free conditions, was estimated to be $11 \pm 5\%$ (Hadiwijaya et al., 2021).
744 In mature boreal forests, 9% to 55% of rainfall can be intercepted by the canopy (Pomeroy et al.,
745 1999). Relevant to deposition of atmospheric constituents, Pomeroy et al. (1999) also reported that
746 up to 70% of intercepted rainfall may evaporate directly from the canopy, which can leave behind
747 non-volatile rainfall solutes. Wet deposition that undergoes stemflow (SF) proceeds down the
748 branches, stems, and/or trunks of a plant, transferring precipitation and nutrients from the canopy
749 to the soil at the trunk or stem base (Ciruzzi and Loheide, 2021). These known mechanisms of
750 canopy interception ultimately reduce the amount of precipitation reaching the ground as TF, and
751 thus, this explains the smaller volumes found in our samplers compared to the OF measured
752 simultaneously. In contrast, the fractions that ranged from 108% to 424%, averaging 186%,
753 demonstrates a different aspect of the highly dynamic nature of canopies where they can sometimes
754 intercept rainfall like an impermeable surface to act as a funnel, guiding large volumes of
755 precipitation on to the ground, or in this case into the TF samplers (Metzger et al., 2019).



757
 758 **Figure 4.** Average volume collected from replicate automated samplers deployed from June 2015
 759 to October 2016, from north (N) to south (S), at the NL-BELT field sites: (a) ER, (b) SR, (c) PB,
 760 and (d) GC. The red trace represents open fall, teal for throughfall, and light green for total
 761 deposition (the sum of conductive and non-conductive precipitation). The total precipitation
 762 volumes depicted for PB, from July 2015 to November 2015, were collected at the nearby HR site
 763 in the same watershed since no total deposition measurements were in place at PB during this
 764 period. The missing volume for GC in 2015 was estimated from the determined ECCC station
 765 linear relationship and is presented as a broken line. The fraction of precipitation collected as open
 766 fall or throughfall, compared to the total deposition (right axis), are represented by diamonds of
 767 the corresponding color. Error bars represent the standard deviation of three measurements from
 768 replicate samples. The axis break spans the winter months when the off-grid automated samplers
 769 were stored.

770

771 3.4 Characterizing Chemical Parameters from NL-BELT

772 In addition to assessing physical parameters, chemical parameters were also evaluated in
 773 this work. Conductivity and pH are measurements commonly made on precipitation samples
 774 collected from the field and so incorporating them into our analysis is useful for instrumental
 775 validation. Additionally, with increasing recognition of their importance as a proxy for ROC
 776 estimation, and in biogeochemical carbon budget closure, DOC flux measurements were used to
 777 compare against a limited number of prior reports, each using different sampling or data
 778 interpretation strategies. These chemical measurements were also made in an underrepresented

779 part of the world in terms of atmospheric deposition sampling and are useful additions to the
780 overarching study of precipitation chemistry.

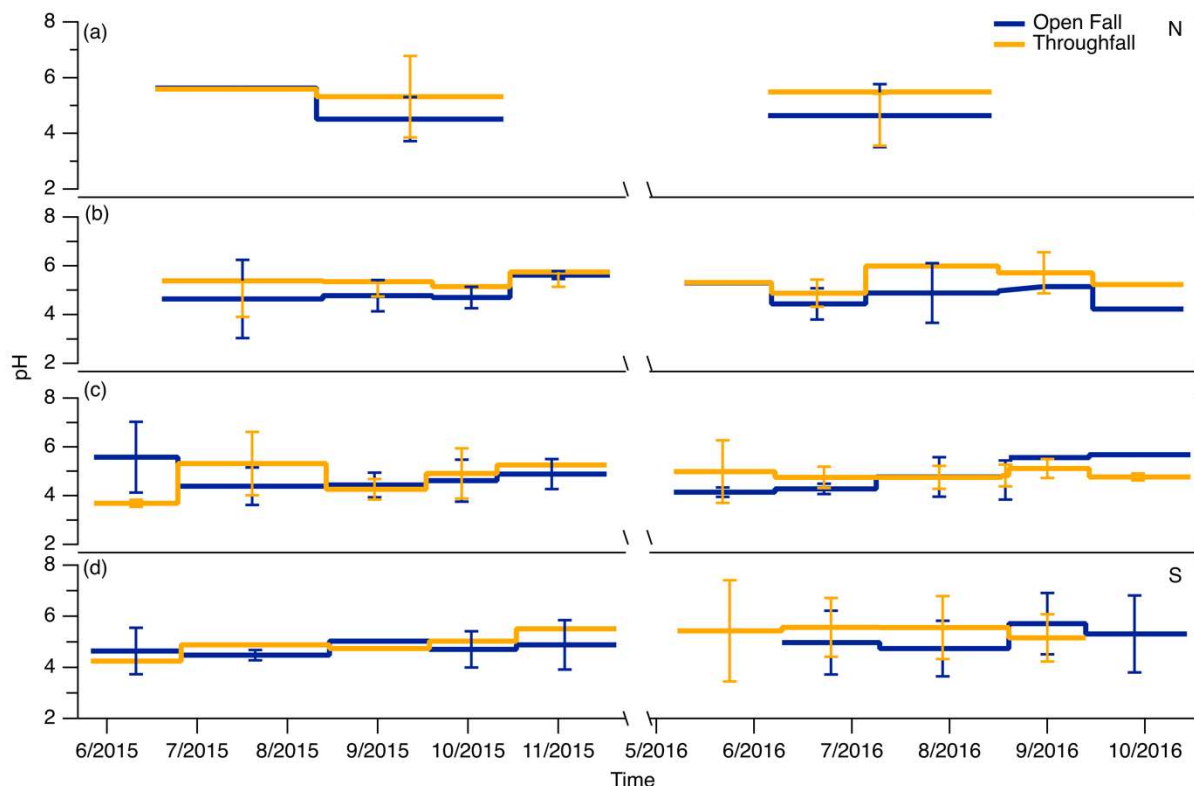
781

782 **3.4.1 Precipitation pH**

783 The deposition of atmospherically persistent pollutants and biogeochemically relevant species
784 to the Earth's surface, or even NO_3^- and SO_4^{2-} historically, can affect the environmental health of
785 soil, air, and water. With the pH range of natural rainwater in equilibrium with atmospheric CO_2
786 expected to be between 5.0 to 5.6, acid rain is defined by values lower than this (Han et al., 2019).
787 Traditionally, the extent of acidity depended on the intercepted atmospheric concentrations of
788 HNO_3 and H_2SO_4 . In any case, monitoring acidity and deposition is especially relevant in remote
789 regions, where major uncertainties and gaps in deposition measurements and global ion
790 concentrations exist (Escarré et al., 1999; Vet et al., 2014). A change in pH can modify the
791 chemical state of many pollutants, altering their transport, bioavailability, and solubility (Guinotte
792 and Fabry, 2008). For example, this can increase exposure and toxicity of metals and nutrients in
793 marine habitats which can go undetected for longer periods in remote areas.

794 Most TF samples were observed to have slightly higher pH than those from OF which had pH
795 values ranging from 4.14 to 5.71 (Figure 5, Table 1). The TF precipitation pH, on average, ranged
796 from 4.74 to 5.99 with rare exceptions falling outside of that range (e.g., July and September 2015
797 PB pH of 3.69 and 4.26, respectively, and the July 2015 GC with pH of 4.12). Excluding these
798 exceptions, there are no major variations observed spatially between the four sites, or temporally
799 between seasons or years (Figure 5). The pH values reported at each of the NL-BELT field sites
800 are comparable to recent OF measurements made at CAPMoN sites in Nova Scotia and
801 Newfoundland and Labrador, where the reported pH of precipitation ranged from 4.44 to 5.19
802 (Houle et al., 2022). The more basic TF overall is expected, as it has been found that up to 90% of
803 H_3O^+ in precipitation can be absorbed by leaves while passing through the canopy (Cappellato et
804 al., 1993). Foliar leaching, the release of ions from leaves, has been commonly reported for base
805 cations such as Mg^{2+} , K^+ , and Ca^{2+} while being minimally observed for other ions such as Cl^- and
806 SO_4^{2-} (Carlson et al., 2003). Mechanisms for foliar leaching include passive cation exchange of
807 H_3O^+ with, for example, cells in the interior of the leaf (Burkhardt and Drechsel, 1997).
808 Additionally, alkaline dust – deposited on the leaves of the canopy, can decrease the acidity of TF
809 precipitation. Such dust can accumulate on leaf surfaces as a result of anthropogenic (i.e., industrial

810 processes) or natural (i.e., wind erosion) sources (Csavina et al., 2012), so that precipitation
 811 passing through the canopy can interact with it (e.g., CaCO_3); thus, neutralizing acidic species and
 812 increasing the TF pH observed in our automated samplers.
 813



814
 815 **Figure 5.** Average pH values from replicate samples collected at each NL-BELT field site, from
 816 north (N) to south (S), at (a) ER, (b) SR, (c) PB, and (d) GC, from June 2015 to August 2016.
 817 Open fall collections are represented using the solid blue trace whereas the orange trace is the pH
 818 of the precipitation collected as throughfall under the balsam fir canopy.

819
 820 The pH of the collected precipitation appears to be similar in both TF and OF as a function of
 821 time – despite the potential for foliar leaching and dust dissolution in the canopy. The same
 822 chemical components may be setting the pH, as these measurements do not vary much seasonally,
 823 geographically, or temporally. As pH is a long-studied measurement, its purpose in this work was
 824 to validate the sample quality from our described collection approach, rather than drive any
 825 scientific objective. Nevertheless, while the NL-BELT measurements demonstrate a recovery
 826 compared to rainwater pH in 1980s eastern North America – prior to NO_x and SO_2 regulation (pH
 827 from 4.1 to 5.0; Barrie and Hales, 1984), the present-day pH remains lower than expected for
 828 natural rainwater (~5.6; Boyd, 2020). Keeping in mind the successful environmental policies
 829 limiting SO_2 and NO_x , leading to considerable decreases in atmospheric concentrations of H_2SO_4

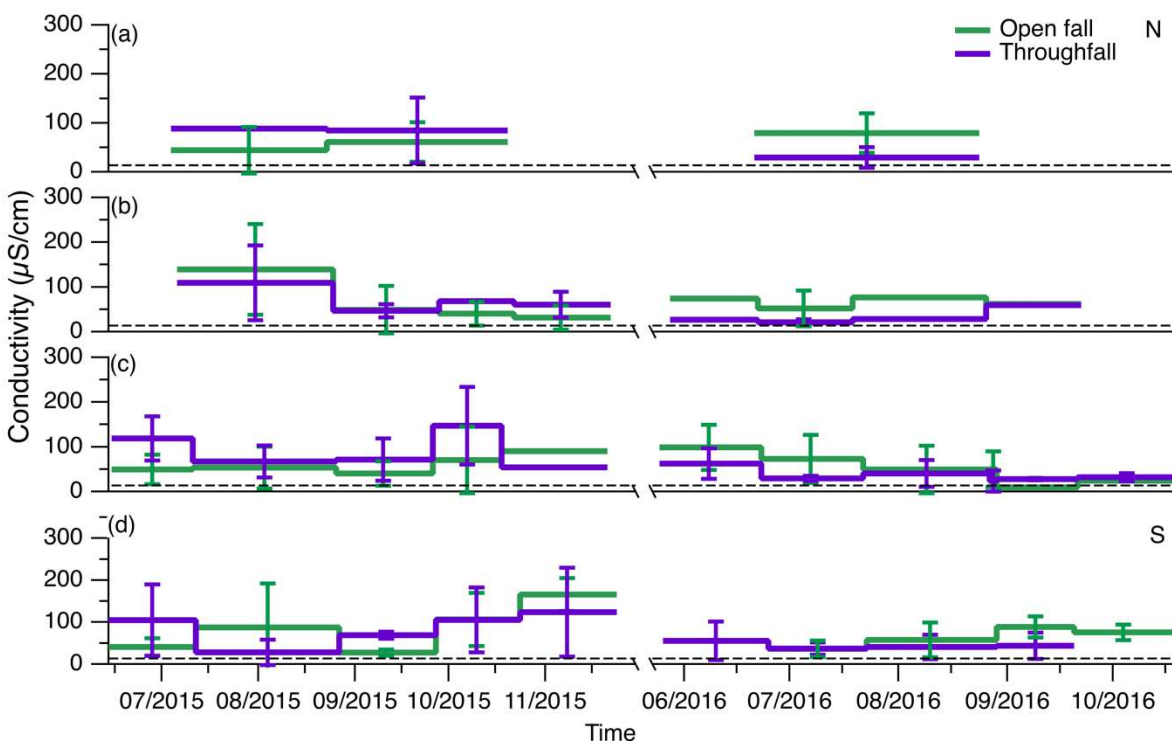
830 and HNO₃, a modern view on the trajectory of continental U.S. cloud water composition and pH
831 has recently been reported (Lawrence et al., 2023). Across the U.S. and eastern Canada,
832 measurements of anion molar charge equivalents have been lower than cations – a potential
833 explanation being an increase in the presence of weak organic acids which commonly have pKa
834 values near 4 (Feng et al., 2021), an outcome we have also observed in aerosol sample chemical
835 composition from Atlantic Canada (Di Lorenzo et al., 2018). With the frequency of acid rain
836 having a pH < 5 decreasing over the past 20 years, these recently reported measurements depict
837 deposition composition shifting away from a ‘linear’ chemical regime dominated by H₃O⁺ and
838 SO₄²⁻ towards a ‘non-linear’ regime designated by low acidity, moderate to high conductivity,
839 potentially weak acid-base buffer systems, and increasing base cation and TOC concentrations
840 (Lawrence et al., 2023). It would seem the evolving chemical contributors to global rainwater pH
841 remain an open line of investigation.

842

843 **3.4.2 Precipitation Conductivity**

844 In all the collected OF and TF precipitation samples, across all four NL-BELT sites, the
845 average measured conductivity values ranged from 21 to 166 μS/cm following no apparent
846 seasonal or temporal trend (Figure 6). Additionally, the conductivity in both OF and TF also
847 appear to vary across the field sites - only within the 2016 TF samples does the conductivity appear
848 to increase with decreasing latitude. Yet, with the typical conductivity of surface and drinking
849 waters being between 1 to 1000 μS/cm (Lin et al., 2017), and typically below 200 μS/cm in stream
850 water measurements within the watersheds of each of the NL-BELT sites, our observations are
851 comparable and fall within the expected range. Our field blanks – encompassing a variety of
852 materials and apparatuses, and our cleaning procedures, routinely produced conductivities of 9 ±
853 5 μS/cm. The conductivity of saturated HgCl₂ in water (at 0.1% vol/vol) was 13.6 ± 0.4 μS/cm,
854 which is also comparable to but statistically higher than our field blanks (p = 0.0015; unpaired t
855 test) and less than what was observed for our samples (p < 2 × 10⁻⁶ for each site considered
856 separately and also across all sites; unpaired t-test). Even with this background correction applied,
857 the conductivity values presented here are expected to be similar to or higher than what would
858 typically be found in rainwater (4 to 150 μS/cm; Beverland et al., 1997) as the rain sensor
859 deliberately selects for precipitation containing ionic chemical components with conductivity
860 greater than 1.0 μS/cm, while excluding pure water during atmospheric washout, which would

861 dilute the dissolved solutes in the wet deposition sample and lower the resulting conductivity
 862 values. The overall comparability between our range and those previously reported, where the
 863 lower limit is slightly higher in our dataset, demonstrates that the principle of operation of our
 864 instrument is robust. It decisively collects precipitation with the property of conductance indicating
 865 dissolved ionic solutes of interest to atmospheric chemical processes.
 866



867
 868 **Figure 6.** Average conductivity measured from replicate automated samplers at the NL-BELT
 869 field sites, from north (N) to south (S), at (a) ER, (b) SR, (c) PB, and (d) GC, from June 2015 to
 870 October 2016. The green trace represents open fall samplers whereas the purple trace represents
 871 throughfall samples. The error bar represents the standard deviation between replicate
 872 measurements. The dashed black line represents the upper threshold of conductivity (13.6 $\mu\text{S}/\text{cm}$)
 873 that arises due when an addition of saturated aqueous HgCl_2 is made to microbially sterilize
 874 samples. Note that all samples have conductivities equivalent to or higher than 13.6 $\mu\text{S}/\text{cm}$.
 875

876 3.4.3. Wet Deposition of Dissolved Organic Carbon (DOC) at NL-BELT

877 The concentration of DOC in OF and TF precipitation, across all four sites, ranged from 3
 878 to 46 mg L^{-1} and 5 to 65 mg L^{-1} with averages of $16 \pm 10 \text{ mg L}^{-1}$ and $22 \pm 12 \text{ mg L}^{-1}$, respectively
 879 (Table 3). Concentrations are influenced by the volume collected and are not useful when
 880 discerning deposition trends and/or mechanisms. The concentrations were converted to elemental
 881 fluxes using the volume of precipitation collected, the area of the funnel and the number of

882 sampling days of each sampling period (Figure 7). The total flux for each sample period was
883 summed and reported as an equivalent annual flux with the following units: $\text{mg C m}^{-2} \text{ a}^{-1}$. Annual
884 fluxes ranged from 600 to 4200 $\text{mg C m}^{-2} \text{ a}^{-1}$ across the study sites for the snow free period (Table
885 S4).

886 The TF DOC fluxes were enhanced compared to the corresponding OF samples as
887 precipitation was intercepted by the forest canopy, with fluxes higher in TF samples by 600, 400,
888 and 400 $\text{mg C m}^{-2} \text{ a}^{-1}$ at GC, SR, and ER, respectively (Table S5). The accumulation of water-
889 soluble organics on forest canopies that increases DOC detected in TF could originate in part from
890 organic carbon-containing compounds aged through oxidation reactions in the atmosphere, which
891 increases their water solubility and propensity for surface interactions. In periods without
892 substantial rain, these oxidized organics deposit effectively to the high surface area of forest
893 canopies, contributing to the elevated DOC measured in TF. Additionally, non-volatile organics
894 left behind from evaporated precipitation intercepted by the canopy could also contribute.
895 Conversely, other mechanisms within the forest could result in enhanced DOC in TF. Recently,
896 Cha et al. (2023) utilized a mass balance approach to determine whether DOC deposition is driven
897 by canopy leaching (i.e., soluble tree resin, leaf exudates, internal tissues and microbes) or
898 dissolution of dry deposited gases and $\text{PM}_{2.5}$ on plant foliage into rainwater. It was found that
899 canopy leaching is the major contributor to TF DOC, accounting for ~83% of throughfall DOC.
900 Whereas, $\text{PM}_{2.5}$ and rainwater only accounted for ~3 and 14%, respectively, while dry deposited
901 gases were not considered. This suggests that internal cycling of DOC within the forest could be
902 an important source of DOC to the throughfall soil interface (Cha et al., 2023). It is possible that a
903 similar mechanism may be responsible for the elevated levels of DOC in TF at the NL-BELT sites,
904 but we cannot explicitly distinguish between internal cycling versus external deposition in the
905 current study.

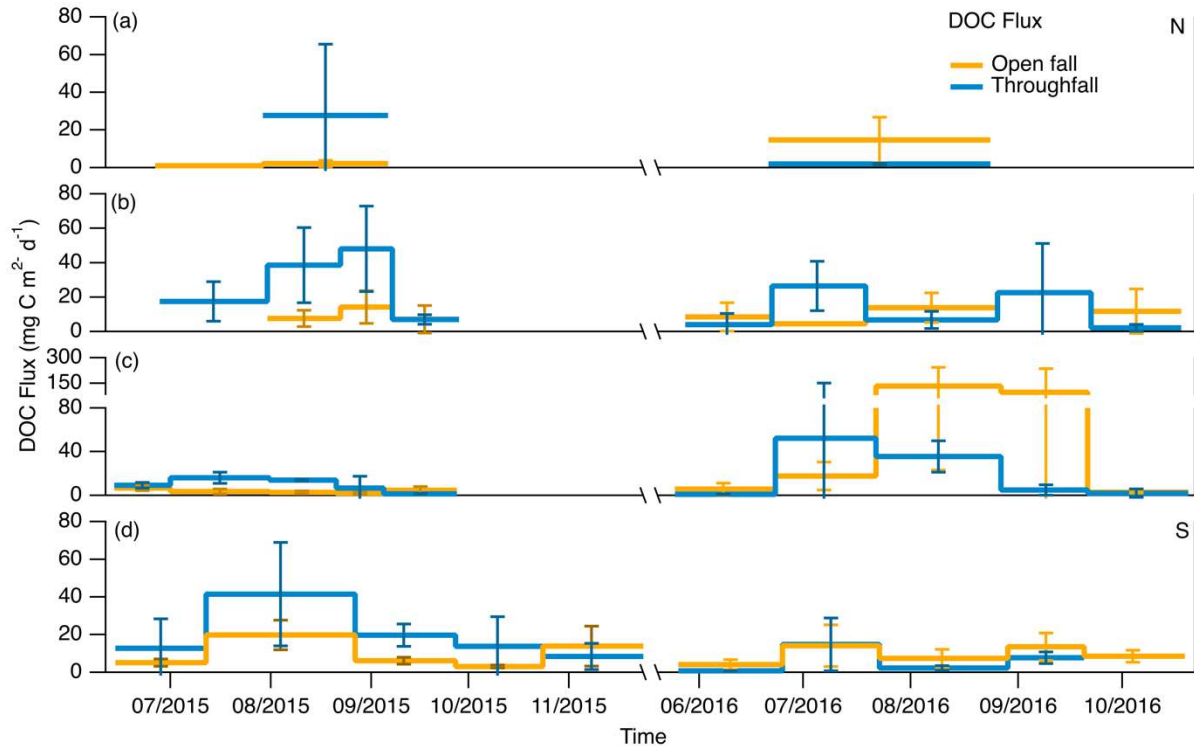
906 A notable exception was observed at PB, where the DOC fluxes in the open fall sample
907 were enhanced up to 1800 $\text{mg C m}^{-2} \text{ a}^{-1}$ when compared to the TF in 2016. This may be attributed
908 to a difference in forest type within this NL-BELT region being black spruce (*Picea mariana*)
909 instead of balsam fir (Bowering et al., 2023). Some studies have suggested that forest type could be
910 a major factor affecting DOC variability (Arisci et al., 2012; Sleutel et al., 2009). Specific
911 differences in canopy height, leaf area index, canopy structure and the shape of leaves and needles
912 could drive DOC differences between forest types (Smith, 1981; Erisman and Draaijers, 2003;

913 Sleutel et al., 2009). The elevated levels in OF samples relative to TF within PB are consistent
914 with idea of uptake and/or leaching of canopy DOC in the internal cycling of DOC, while the
915 enhanced TF at the rest of the sites is more difficult to observational constrain the participating
916 processes.

917 Episodic events, such as polluted air masses from wildfires could also result in elevated
918 deposition of DOC. It is estimated that $\sim 116 - 385 \text{ Tg C a}^{-1}$ is produced globally due to the
919 incomplete combustion of biomass during landscape fires (Santín et al., 2016; Coward et al., 2022).
920 Several studies have associated enhanced DOC levels with wildfires (Gao et al., 2003; Moore,
921 2003; Wonaschütz et al., 2011; Myers-Pigg et al., 2015). More recently, Coward et al. (2022)
922 measured DOC in Pacific surface waters along the California coastline and observed 100 to 400
923 % increases in DOC concentration, when compared to pre-wildfire conditions. It is possible that a
924 similar biomass burning plume that underwent atmospheric washout, could be responsible for the
925 enhancement in the observed DOC at NL-BELT, overlaid on a background more typical of
926 seasonal oxidation of biogenic DOC. This also coincides with the seasonal variability observed in
927 OF samples from the same summer where elevated levels of DOC were measured. For instance,
928 the DOC deposition at PB for August 2016 was 4800 mg C m^{-2} , whereas the total deposition for
929 the same year was $7800 \text{ mg C m}^{-2} \text{ a}^{-1}$. This single period accounts for 62% of the total DOC
930 deposition at this site. This underscores the pivotal role that episodic transport may play in
931 influencing the dynamics of DOC deposition, particularly with a warming future where wildfires
932 are more prevalent.

933 The deposition trend observed in the current study also highlights the complexity of the
934 varied drivers of atmospheric ROC, in which some months have more DOC in TF versus OF and
935 occasionally the opposite is observed. Generally, we observed similar fluxes in both samples –
936 suggesting that the amount of deposited carbon is comparable. Although the volume of
937 precipitation captured in TF samplers are generally lower when compared to the corresponding
938 OF samplers, the deposition flux of DOC is greater in TF samplers. With DOC enhanced in TF
939 samples, the values reported here could be an underestimation of the amount of carbon reaching
940 the forest floor during precipitation events due to competing processes within the canopy. One
941 such process is stemflow (SF), where a fraction of precipitation intercepted by the forest canopy
942 is funneled over the bark of the tree surface to the base of the tree stem (Oka et al., 2021). Although,
943 SF was not measured in the current study, several studies have demonstrated that DOC

944 concentrations are enhanced in SF when compared to the corresponding TF and bulk precipitation
 945 samples (Stubbins et al., 2017; Van Stan and Stubbins, 2018; Ryan et al., 2021). Additionally, we
 946 cannot rule out that the chemical speciation differs between OF, TF, and SF even if the DOC values
 947 are similar, but such insights require more selective instrumentation for chemical analysis (e.g.,
 948 high resolution mass spectrometry).
 949



950
 951 **Figure 7.** Average DOC fluxes ($\text{mg C m}^{-2} \text{d}^{-1}$) in replicate samples collected at the NL-BELT field sites, from north (N) to south (S), at (a) ER, (b) SR, (c) PB, and (d) GC, from June 2015 to August
 952
 953
 954
 955
 956
 957
 958

959 The ability to accurately determine DOC in OF and TF precipitation demonstrates the
 960 capability of the automated deposition samplers. To validate our measurements, we compared our
 961 observed fluxes to other studies in different forest types. Mean annual DOC fluxes were generally
 962 similar to those reported in some other boreal forests (Table 3). These include Finland, with work
 963 in stands that consisted mainly of Scots pine (*Pinus sylvestris L.*) (mean OF 2.32; TF, 4.35 $\text{g C m}^{-2} \text{a}^{-1}$;
 964 Pumpanen et al., 2014), as well as in Mont St. Hilarie, Québec (mean OF 0.49; TF 2.05 $\text{g C m}^{-2} \text{a}^{-1}$;
 Dalva and Moore, 1991), which also consisted of a variety of tree species such as yellow

965 birch (*Betula allenganien*), red maple (*Acer rubrum*), and sugar maple (*Acer saccharum*).
966 Conversely, the annual fluxes were orders of magnitude lower than measurements made at the
967 University of Georgia (23 to 48 g C m⁻² a⁻¹) which has a subtropic climate consisting mainly of
968 southern live oak (*Quercus virginiana Mill.*) and eastern red cedar (*Juniperus virginiana L.*)
969 occasionally hosting dense epiphytes (Van Stan et al., 2017). This highlights the potential
970 variability to expect when measuring DOC in different forest systems, as the annual DOC fluxes
971 vary depending on factors such as climate, tree species composition, and environmental conditions.

972 These results underscore the pivotal role the off-grid custom-built automated deposition
973 samplers can play in advancing scientific research, particularly in precipitation monitoring and
974 analysis. The automated system enabled long term continuous sample collection in remote
975 locations, which was previously challenging to attain due to the need for frequent human
976 intervention and resources required to regularly access these experimental forest stands. These
977 samplers also allowed us to compare DOC through replicate measurements in TF and OF samples
978 which sheds light on the potentially different DOC deposition chemistries within the NL-BELT
979 region. The automated system better maintains the integrity of DOC in the samples. This was
980 achieved by following standard procedures for biogeochemical sample preservation (i.e., adding
981 HgCl₂) (Argentino et al., 2023), employing a rigorous cleaning procedure, and preventative design
982 against the intrusion of forest litter which could result in a positive bias for DOC in the collected
983 precipitation. The use of replicates also results in more robust scientific conclusions and broader
984 applicability of the results, and they can be obtained for a fraction of the cost of a commercial
985 equivalent, highlighting the contribution these automated systems are capable of when applied to
986 current precipitation monitoring. As a result, these samplers show promise in the quantification of
987 biogeochemical and anthropogenic chemical species of interest, which will be visited in future
988 manuscripts drawing from the samples presented in this dataset, and others since obtained, but are
989 beyond the scope of this manuscript in demonstrating the performance of this new instrumentation.

990

991

992

993

994

995

996

997 **Table 3.** Concentrations (mg C L^{-1}) and annual fluxes ($\text{g C m}^{-2} \text{a}^{-1}$) of DOC in precipitation (P),
 998 open fall (OF), throughfall (TF), and stemflow (SF) collected at forested sites. Where volumes are
 999 not available for other studies, fluxes are not possible to calculate. The values reported in the
 1000 current study are the estimated DOC flux for the wet deposition sampling period (~June through
 1001 October) for each year and therefore represents the lower limit of DOC deposition, as the dataset
 1002 excludes snow.

Site	Type	Mean Concentration (mg C L^{-1})	Annual Flux ($\text{g C m}^{-2} \text{a}^{-1}$)	References
Grand Codroy, NL, Canada (2015 to 2016)	OF	12.83	1.56	This study
	TF	23.40	2.20	
Pynn's Brook, NL, Canada (2015 to 2016)	OF	19.98	4.21	
	TF	21.24	2.44	
Salmon River, NL, Canada (2015 to 2016)	OF	16.14	1.33	
	TF	21.00	2.65	
Eagle River, NL, Canada (2015 to 2016)	OF	11.59	0.53	
	TF	28.26	0.86	
Mont St. Hilaire, QC, Canada (1987)	P	2.00	0.49	Dalva and Moore, 1991
	TF	12.13	2.05	
	SF	40.10	0.10	
Northern China (2007 to 2008)	P	2.4 to 3.9	1.4 to 2.7	Pan et al., 2010
Coulissenhieb, Northeast Bavaria (1995 to 1997)	P	2.70	-	Michalzik and Matzner, 1999
	TF	15.20	-	
Hobcaw Barony, South Carolina, USA (2014 to 2015)	P	1.20	-	Chen et al., 2019
	Pine TF	26.00	-	
	Oak TF	38.8	-	
University of Georgia, USA 2015 to 2016	TF Epiphyte Oak	17	23**	Van Stan et al., 2017
	TF Bare Cedar	20	32**	
	TF Epiphyte Cedar	54	48**	
SMEARII Site, Southern Finland (1998 to 2012)	P	3.24	2.32	Pumpanen et al., 2014
	TF	10.10	4.35	

** Estimated DOC yield for 2016 ($\text{g C m}^{-2} \text{a}^{-1}$) where sampled storms values (g C event^{-1}) were scaled to an annual deposition value using meteorological data and a linear rainfall-DOC yield relationship.

1003
 1004
 1005
 1006

1007 **4.0 Conclusions and Future Directions**

1008 This paper presents a cost-effective automated deposition sampler for continuous
1009 collection of precipitation. An open-source procedure and schematics for building these samplers
1010 is provided alongside the rationale for selecting the materials in the current study to target analytes
1011 of scientific interest in wet deposition samples. These low-power systems are demonstrated in
1012 being capable of continuous off-grid use for sample collection over two years at the NL-BELT
1013 experimental sites, with replacement of battery power packs monthly or bimonthly, with on-grid
1014 performance also provided for comparison. The resulting systems enhance the accessibility of
1015 automated wet deposition samplers to scientists globally and this work highlights their robust
1016 performance in collecting and preserving rainwater conductivity and pH, alongside providing
1017 measurements of DOC from this understudied region that builds a broader picture of the
1018 atmosphere-surface exchange of this biogeochemical pool across the NL-BELT. Comparability
1019 and complementarity of our results to well-established and current measurements of interest like
1020 DOC, demonstrate their efficacy and potential application to the study of processes such as
1021 canopy-precipitation interactions through the collection of open fall and throughfall replicates. The
1022 capacity to autonomously collect wet deposition, in addition to traditional bulk deposition samples
1023 can shed light on competing wet and dry deposition processes. Should on-grid capacity suit
1024 scientific objectives, these samplers are anticipated to be possible for use year-round when paired
1025 with more power-intensive strategies to facilitate solid to liquid phase transfer for detected and
1026 collected precipitation in the winter.

1027 For the broader deposition-motivated community, the instrument design also allows for
1028 easy cost-effective modification of the number of replicate samplers, the material composition of
1029 all surfaces the aqueous samples interact with, as well as preservation strategies - depending on
1030 the analyte of interest. For example, the lack of organic nitrogen measurements within universally
1031 established sampling and measurement procedures serves as a general example of the substantial
1032 knowledge gaps that may result when translating limited data sets to the wider global picture. This
1033 includes incomplete speciation and quantification across precipitation, aerosol, and gas phases.
1034 Monitoring systems that support U.S. deposition assessments (e.g., the NADP) only characterize
1035 the inorganic fraction of wet deposition. Additionally, modern emerging issues that require the
1036 continuation of existing deposition measurements or expansion of observation programs revolve
1037 around identifying and quantifying compound classes of concern, such as persistent organic

1038 pollutants. As reported in the literature, the deposition of these types of pollutants (e.g.,
1039 polychlorinated biphenyls, polycyclic aromatic hydrocarbons, etc.) can be monitored using
1040 suitable collectors made of amber-coloured glass or stainless steel (Fingler et al., 1994; Amodio et
1041 al., 2014) - modifications which can be applied to the sample design detailed here. The samples
1042 collected in this work from this new instrumentation, specifically, are expected to be used further
1043 in several upcoming complementary and novel environmental monitoring studies. Not only will
1044 this future work extend our biogeochemical analysis, but it will also assist in our studying of the
1045 transport of other anthropogenic pollutants of emerging interest which are beyond the scope of
1046 describing this new platform.

1047

1048 *Data availability.* The sampler performance and precipitation properties measurements (pH,
1049 conductivity, and DOC) can be found in Colussi et al. (2024, <https://doi.org/XXXX>). The data are
1050 available from the corresponding author (TV) on request.

1051

1052 *Author contributions.* AC, DP, and ML performed the data analysis. AC and DP wrote the
1053 manuscript with contributions from all authors. Sampler design and construction were led by TV,
1054 with assistance from BP and RH for initial prototypes, DP and ML for the revised iteration, and
1055 AC for the final modular control boards. Sample collection and associated characterization
1056 measurements were performed by BP and TV. Conceptualization and conduct of the sampling
1057 experiments were made by TV, CY, KE, and SZ. All authors were involved in examining and
1058 reviewing the results. All authors were involved in editing the paper.

1059

1060 *Competing interests.* The contact author has declared that none of the authors has any competing
1061 interests.

1062

1063 **5.0 Acknowledgements**

1064 Funding for this work was provided by the Newfoundland and Labrador Department of
1065 Agrifoods and Forestry, Centre for Forestry Science and Innovation (Project 221269), and the
1066 Harris Centre at Memorial University. T. C. VandenBoer was supported for this work in-part
1067 through a Government of Canada Banting Postdoctoral Fellowship. Fieldwork sample collection
1068 by B. K. Place was supported by funding from Polar Knowledge Canada through the Northern
1069 Scientific Training Program. Additional financial support for full redesign of the samplers was
1070 provided through Environment and Climate Change Canada Grants & Contributions

1071 (GCXE20S009). A. A. Colussi acknowledges support for this work through a Natural Sciences
1072 and Engineering Research Council of Canada (NSERC) Graduate Scholarship – Master’s program
1073 (CGSM) and Ontario Graduate Scholarship (OGS). M. Lao acknowledges support for this work
1074 through a NSERC Undergraduate Student Research Award (USRA). We thank C. M. Laprise and
1075 C. Conlan for aid in the collection and organization of samples for analysis, supported in part by
1076 the Memorial University Career Experience Program (MUCEP) and V. Sitahai through a York
1077 University Dean’s Undergraduate Research Award (DURA). T. C. VandenBoer, C. J. Young and
1078 S. E. Ziegler were supported through the NSERC Discovery (RGPIN-2020-06166; RGPIN-2018-
1079 05990; RGPIN-2018-05383) and Strategic Partnerships (479224) Programs. The authors would
1080 also like to thank B. Hearn, D. Harris, A. Skinner, C. Young, J. J. MacInnis, J. Warren, and L.
1081 Souza for their invaluable assistance in sampling site access and set up, off-season storage of
1082 collection units, sample collection and analysis, and meteorological reanalysis. We thank H. Hung
1083 and C. Shunthirasingham for productive discussions on modular design and considerations for
1084 collection of persistent pollutants.

1085

1086 **6.0 References**

1087 Amodio, M., Catino, S., Dambruoso, P. R., de Gennaro, G., Di Gilio, A., Giungato, P., Laiola, E.,
1088 Marzocca, A., Mazzone, A., Sardaro, A., and Tutino, M.: Atmospheric Deposition: Sampling
1089 Procedures, Analytical Methods, and Main Recent Findings from the Scientific Literature, *Adv.*
1090 *Meteorol.*, 2014, 161730, <https://doi.org/10.1155/2014/161730>, 2014.

1091 Argentino, C., Kalenitchenko, D., Lindgren, M., and Panieri, G.: HgCl₂ addition to pore water
1092 samples from cold seeps can affect the geochemistry of dissolved inorganic carbon ([DIC],
1093 $\delta^{13}\text{CDIC}$), *Mar. Chem.*, 251, 104236, <https://doi.org/10.1016/j.marchem.2023.104236>, 2023.

1094 Arisci, S., Rogora, M., Marchetto, A., and Dichiaro, F.: The role of forest type in the variability of
1095 DOC in atmospheric deposition at forest plots in Italy, *Environ. Monit. Assess.*, 184, 3415–3425,
1096 <https://doi.org/10.1007/s10661-011-2196-2>, 2012.

1097 Audoux, T., Laurent, B., Desboeufs, K., Noyalet, G., Maisonneuve, F., Lauret, O., and Chevaillier,
1098 S.: Intra-event evolution of elemental and ionic concentrations in wet deposition in an urban
1099 environment, *Atmospheric Chem. Phys.*, 23, 13485–13503, [https://doi.org/10.5194/acp-23-](https://doi.org/10.5194/acp-23-13485-2023)
1100 [13485-2023](https://doi.org/10.5194/acp-23-13485-2023), 2023.

1101 Avery, G. B., Willey, J. D., and Kieber, R. J.: Carbon isotopic characterization of dissolved organic
1102 carbon in rainwater: Terrestrial and marine influences, *Atmos. Environ.*, 40, 7539–7545,
1103 <https://doi.org/10.1016/j.atmosenv.2006.07.014>, 2006.

- 1104 Barber, V. P. and Kroll, J. H.: Chemistry of Functionalized Reactive Organic Intermediates in the
1105 Earth's Atmosphere: Impact, Challenges, and Progress, *J. Phys. Chem. A*, 125, 10264–10279,
1106 <https://doi.org/10.1021/acs.jpca.1c08221>, 2021.
- 1107 Barrie, L. A. and Hales, J. M.: The spatial distributions of precipitation acidity and major ion wet
1108 deposition in North America during 1980, *Tellus B Chem. Phys. Meteorol.*, 36, 333–355,
1109 <https://doi.org/10.3402/tellusb.v36i5.14915>, 1984.
- 1110 Beverland, I. J., Heal, M. R., Crowther, J. M., and Srinivas, M. S. N.: Real-time measurement and
1111 interpretation of the conductivity and pH of precipitation samples, *Water. Air. Soil Pollut.*, 98,
1112 325–344, <https://doi.org/10.1007/BF02047042>, 1997.
- 1113 Bowering, K. L., Edwards, K. A., Wiersma, Y. F., Billings, S. A., Warren, J., Skinner, A., and
1114 Ziegler, S. E.: Dissolved Organic Carbon Mobilization Across a Climate Transect of Mesic Boreal
1115 Forests Is Explained by Air Temperature and Snowpack Duration, *Ecosystems*, 26, 55–71,
1116 <https://doi.org/10.1007/s10021-022-00741-0>, 2022.
- 1117 Bowering, K. L., Edwards, K. A., and Ziegler, S. E.: Seasonal controls override forest harvesting
1118 effects on the composition of dissolved organic matter mobilized from boreal forest soil organic
1119 horizons, *Biogeosciences*, 20, 2189–2206, <https://doi.org/10.5194/bg-20-2189-2023>, 2023.
- 1120 Bowyer, Peter J. (Ed.): *Where the Wind Blows: A Guide to Marine Weather in Atlantic Canada*,
1121 Breakwater Books Ltd., St John's, Newfoundland, 53 pp., 1995.
- 1122 Boyd, C. E.: Carbon Dioxide, pH, and Alkalinity, in: *Water Quality: An Introduction*, edited by:
1123 Boyd, C. E., Springer International Publishing, Cham, 177–203, https://doi.org/10.1007/978-3-030-23335-8_9, 2020.
- 1125 Brahney, J., Wetherbee, G., Sexstone, G. A., Youngbull, C., Strong, P., and Heindel, R. C.: A new
1126 sampler for the collection and retrieval of dry dust deposition, *Aeolian Res.*, 45, 100600,
1127 <https://doi.org/10.1016/j.aeolia.2020.100600>, 2020.
- 1128 Burkhardt, J. and Drechsel, P.: The synergism between SO₂ oxidation and manganese leaching on
1129 spruce needles — A chamber experiment, *Environ. Pollut.*, 95, 1–11,
1130 [https://doi.org/10.1016/S0269-7491\(96\)00126-1](https://doi.org/10.1016/S0269-7491(96)00126-1), 1997.
- 1131 Canadian Air and Precipitation Monitoring Network: Inspector's Reference Manual -
1132 Precipitation, 1985.
- 1133 Cappellato, R., Peters, N. E., and Ragsdale, H. L.: Acidic atmospheric deposition and canopy
1134 interactions of adjacent deciduous and coniferous forests in the Georgia Piedmont, *Can. J. For.*
1135 *Res.*, 23, 1114–1124, <https://doi.org/10.1139/x93-142>, 1993.
- 1136 Carlson, J., Gough, W. A., Karagatzides, J. D., and Tsuji, L. J. S.: Canopy Interception of Acid
1137 Deposition in Southern Ontario, *Can. Field-Nat.*, 117, 523–530,
1138 <https://doi.org/10.22621/cfn.v117i4.799>, 2003.

- 1139 Casas-Ruiz, J. P., Bodmer, P., Bona, K. A., Butman, D., Couturier, M., Emilson, E. J. S., Finlay,
1140 K., Genet, H., Hayes, D., Karlsson, J., Paré, D., Peng, C., Striegl, R., Webb, J., Wei, X., Ziegler,
1141 S. E., and del Giorgio, P. A.: Integrating terrestrial and aquatic ecosystems to constrain estimates
1142 of land-atmosphere carbon exchange, *Nat. Commun.*, 14, 1571, [https://doi.org/10.1038/s41467-](https://doi.org/10.1038/s41467-023-37232-2)
1143 [023-37232-2](https://doi.org/10.1038/s41467-023-37232-2), 2023.
- 1144 Cha, J.-Y., Lee, S.-C., Lee, E.-J., Lee, K., Lee, H., Kim, H. S., Ahn, J., and Oh, N.-H.: Canopy
1145 Leaching Rather than Desorption of PM_{2.5} From Leaves Is the Dominant Source of Throughfall
1146 Dissolved Organic Carbon in Forest, *Geophys. Res. Lett.*, 50, e2023GL103731,
1147 <https://doi.org/10.1029/2023GL103731>, 2023.
- 1148 Chen, H., Tsai, K.-P., Su, Q., Chow, A. T., and Wang, J.-J.: Throughfall Dissolved Organic Matter
1149 as a Terrestrial Disinfection Byproduct Precursor, *ACS Earth Space Chem.*, 3, 1603–1613,
1150 <https://doi.org/10.1021/acsearthspacechem.9b00088>, 2019.
- 1151 Ciruzzi, D. M. and Loheide, S. P.: Monitoring Tree Sway as an Indicator of Interception Dynamics
1152 Before, During, and Following a Storm, *Geophys. Res. Lett.*, 48, e2021GL094980,
1153 <https://doi.org/10.1029/2021GL094980>, 2021.
- 1154 Colli, M., Lanza, L. G., Rasmussen, R., and Thériault, J. M.: The Collection Efficiency of Shielded
1155 and Unshielded Precipitation Gauges. Part II: Modeling Particle Trajectories, *J. Hydrometeorol.*,
1156 17, 245–255, <https://doi.org/10.1175/JHM-D-15-0011.1>, 2016.
- 1157 Colussi, A. A., Persaud, D., Lao, M. Place, B. K., Hems, R. F., Ziegler, S. E., Edwards, K. A.,
1158 Young, C. J., and VandenBoer, T. C.: Off-grid automatic precipitation measurements of pH,
1159 conductivity, and dissolved organic carbon across the Newfoundland and Labrador Boreal
1160 Ecosystem Latitudinal Transect. Federated Research Data Repository [data set]. doi: **XXXXXX**
- 1161 Coward, E. K., Seech, K., Carter, M. L., Flick, R. E., and Grassian, V. H.: Of Sea and Smoke:
1162 Evidence of Marine Dissolved Organic Matter Deposition from 2020 Western United States
1163 Wildfires, *Environ. Sci. Technol. Lett.*, 9, 869–876, <https://doi.org/10.1021/acs.estlett.2c00383>,
1164 2022.
- 1165 Csavina, J., Field, J., Taylor, M. P., Gao, S., Landázuri, A., Betterton, E. A., and Sáez, A. E.: A
1166 review on the importance of metals and metalloids in atmospheric dust and aerosol from mining
1167 operations, *Sci. Total Environ.*, 433, 58–73, <https://doi.org/10.1016/j.scitotenv.2012.06.013>, 2012.
- 1168 Dalva, M. and Moore, T. R.: Sources and sinks of dissolved organic carbon in a forested swamp
1169 catchment, *Biogeochemistry*, 15, 1–19, <https://doi.org/10.1007/BF00002806>, 1991.
- 1170 Di Lorenzo, R. A., Place, B. K., VandenBoer, T. C., and Young, C. J.: Composition of Size-
1171 Resolved Aged Boreal Fire Aerosols: Brown Carbon, Biomass Burning Tracers, and Reduced
1172 Nitrogen, *ACS Earth Space Chem.*, 2, 278–285,
1173 <https://doi.org/10.1021/acsearthspacechem.7b00137>, 2018.
- 1174 Dossett, S. R. and Bowersox, V. C.: National Trends Network Site Operation Manual, 1999.

- 1175 Eaton, J. S., Likens, G. E., and Bormann, F. H.: Throughfall and Stemflow Chemistry in a Northern
1176 Hardwood Forest, *J. Ecol.*, 61, 495–508, <https://doi.org/10.2307/2259041>, 1973.
- 1177 Erisman, J. W. and Draaijers, G.: Deposition to forests in Europe: most important factors
1178 influencing dry deposition and models used for generalisation, *Environ. Pollut.*, 124, 379–388,
1179 [https://doi.org/10.1016/S0269-7491\(03\)00049-6](https://doi.org/10.1016/S0269-7491(03)00049-6), 2003.
- 1180 Escarré, A., Carratalá, A., Àvila, A., Bellot, J., Piñol, J., and Milán, M.: Precipitation Chemistry
1181 and Air Pollution, in: *Ecology of Mediterranean Evergreen Oak Forests*, edited by: Rodà, F.,
1182 Retana, J., Gracia, C. A., and Bellot, J., Springer Berlin Heidelberg, Berlin, Heidelberg, 195–208,
1183 https://doi.org/10.1007/978-3-642-58618-7_14, 1999.
- 1184 Farmer, D. K., Boedicker, E. K., and DeBolt, H. M.: Dry Deposition of Atmospheric Aerosols:
1185 Approaches, Observations, and Mechanisms, *Annu. Rev. Phys. Chem.*, 72, 375–397,
1186 <https://doi.org/10.1146/annurev-physchem-090519-034936>, 2021.
- 1187 Feng, J., Vet, R., Cole, A., Zhang, L., Cheng, I., O'Brien, J., and Macdonald, A.-M.: Inorganic
1188 chemical components in precipitation in the eastern U.S. and Eastern Canada during 1989–2016:
1189 Temporal and regional trends of wet concentration and wet deposition from the NADP and
1190 CAPMoN measurements, *Atmos. Environ.*, 254, 118367,
1191 <https://doi.org/10.1016/j.atmosenv.2021.118367>, 2021.
- 1192 Fingler, S., Tkalčević, B., Fröbe, Z., and Drevenkar, V.: Analysis of polychlorinated biphenyls,
1193 organochlorine pesticides and chlorophenols in rain and snow, *Analyst*, 119, 1135–1140,
1194 <https://doi.org/10.1039/AN9941901135>, 1994.
- 1195 Fowler, D.: Wet and Dry Deposition of Sulphur and Nitrogen Compounds from the Atmosphere,
1196 1980.
- 1197 Galloway, J. N. and Likens, G. E.: The collection of precipitation for chemical analysis, *Tellus*,
1198 30, 71–82, <https://doi.org/10.3402/tellusa.v30i1.10318>, 1978.
- 1199 Gao, S., Hegg, D. A., Hobbs, P. V., Kirchstetter, T. W., Magi, B. I., and Sadilek, M.: Water-soluble
1200 organic components in aerosols associated with savanna fires in southern Africa: Identification,
1201 evolution, and distribution, *J. Geophys. Res. Atmospheres*, 108,
1202 <https://doi.org/10.1029/2002JD002324>, 2003.
- 1203 Gatz, D. F., Selman, R. F., Langs, R. K., and Holtzman, R. B.: An Automatic Sequential Rain
1204 Sampler, *J. Appl. Meteorol.* 1962-1982, 10, 341–344, 1971.
- 1205 George, C.: Photosensitization is in the air and impacts the multiphase on oxidation capacity, 2023.
- 1206 Germer, S., Neill, C., Krusche, A. V., Neto, S. C. G., and Elsenbeer, H.: Seasonal and within-event
1207 dynamics of rainfall and throughfall chemistry in an open tropical rainforest in Rondônia, Brazil,
1208 *Biogeochemistry*, 86, 155–174, <https://doi.org/10.1007/s10533-007-9152-9>, 2007.

- 1209 Grennfelt, P., Engleryd, A., Forsius, M., Hov, Ø., Rodhe, H., and Cowling, E.: Acid rain and air
1210 pollution: 50 years of progress in environmental science and policy, *Ambio*, 49, 849–864,
1211 <https://doi.org/10.1007/s13280-019-01244-4>, 2020.
- 1212 Guinotte, J. M. and Fabry, V. J.: Ocean Acidification and Its Potential Effects on Marine
1213 Ecosystems, *Ann. N. Y. Acad. Sci.*, 1134, 320–342, <https://doi.org/10.1196/annals.1439.013>,
1214 2008.
- 1215 Hadiwijaya, B., Isabelle, P.-E., Nadeau, D. F., and Pepin, S.: Observations of canopy storage
1216 capacity and wet canopy evaporation in a humid boreal forest, *Hydrol. Process.*, 35, e14021,
1217 <https://doi.org/10.1002/hyp.14021>, 2021.
- 1218 Hall, D. J.: Precipitation collector for use in the Secondary National Acid Deposition Network,
1219 United States, 1985.
- 1220 Han, G., Song, Z., Tang, Y., Wu, Q., and Wang, Z.: Ca and Sr isotope compositions of rainwater
1221 from Guiyang city, Southwest China: Implication for the sources of atmospheric aerosols and their
1222 seasonal variations, *Atmos. Environ.*, 214, 116854,
1223 <https://doi.org/10.1016/j.atmosenv.2019.116854>, 2019.
- 1224 Heald, C. L. and Kroll, J. H.: The fuel of atmospheric chemistry: Toward a complete description
1225 of reactive organic carbon, *Sci. Adv.*, 6, <https://doi.org/10.1126/sciadv.aay8967>, 2020.
- 1226 Heald, C. L., Gouw, J. de, Goldstein, A. H., Guenther, A. B., Hayes, P. L., Hu, W., Isaacman-
1227 VanWertz, G., Jimenez, J. L., Keutsch, F. N., Koss, A. R., Misztal, P. K., Rappenglück, B.,
1228 Roberts, J. M., Stevens, P. S., Washenfelder, R. A., Warneke, C., and Young, C. J.: Contrasting
1229 Reactive Organic Carbon Observations in the Southeast United States (SOAS) and Southern
1230 California (CalNex), *Environ. Sci. Technol.*, 54, 14923–14935,
1231 <https://doi.org/10.1021/acs.est.0c05027>, 2020.
- 1232 Houle, D., Augustin, F., and Couture, S.: Rapid improvement of lake acid–base status in Atlantic
1233 Canada following steep decline in precipitation acidity, *Can. J. Fish. Aquat. Sci.*, 79, 2126–2137,
1234 <https://doi.org/10.1139/cjfas-2021-0349>, 2022.
- 1235 Howard, M., Hathaway, J. M., Tirpak, R. A., Lisenbee, W. A., and Sims, S.: Quantifying urban
1236 tree canopy interception in the southeastern United States, *Urban For. Urban Green.*, 77, 127741,
1237 <https://doi.org/10.1016/j.ufug.2022.127741>, 2022.
- 1238 Iavorivska, L., Boyer, E. W., and DeWalle, D. R.: Atmospheric deposition of organic carbon via
1239 precipitation, *Acid Rain Its Environ. Eff. Recent Sci. Adv.*, 146, 153–163,
1240 <https://doi.org/10.1016/j.atmosenv.2016.06.006>, 2016.
- 1241 Jacob, Daniel J.: *Introduction to Atmospheric Chemistry*, Princeton University Press, Princeton,
1242 New Jersey, 49 pp., 1999.
- 1243 Jurado, E., Jaward, F. M., Lohmann, R., Jones, K. C., Simó, R., and Dachs, J.: Atmospheric Dry
1244 Deposition of Persistent Organic Pollutants to the Atlantic and Inferences for the Global Oceans,
1245 *Environ. Sci. Technol.*, 38, 5505–5513, <https://doi.org/10.1021/es049240v>, 2004.

- 1246 Jurado, E., Jaward, F., Lohmann, R., Jones, K. C., Simó, R., and Dachs, J.: Wet Deposition of
1247 Persistent Organic Pollutants to the Global Oceans, *Environ. Sci. Technol.*, 39, 2426–2435,
1248 <https://doi.org/10.1021/es048599g>, 2005.
- 1249 Kattner, G.: Storage of dissolved inorganic nutrients in seawater: poisoning with mercuric
1250 chloride, *Mar. Chem.*, 67, 61–66, [https://doi.org/10.1016/S0304-4203\(99\)00049-3](https://doi.org/10.1016/S0304-4203(99)00049-3), 1999.
- 1251 Kirkwood, D. S.: Stability of solutions of nutrient salts during storage, *Mar. Chem.*, 38, 151–164,
1252 [https://doi.org/10.1016/0304-4203\(92\)90032-6](https://doi.org/10.1016/0304-4203(92)90032-6), 1992.
- 1253 Kochendorfer, J., Meyers, T. P., Hall, M. E., Landolt, S. D., and Diamond, H. J.: A new reference-
1254 quality precipitation gauge wind shield, *Atmospheric Meas. Tech. Discuss.*, 2023, 1–17,
1255 <https://doi.org/10.5194/amt-2023-2>, 2023.
- 1256 Kroll, J. H., Donahue, N. M., Jimenez, J. L., Kessler, S. H., Canagaratna, M. R., Wilson, K. R.,
1257 Altieri, K. E., Mazzoleni, L. R., Wozniak, A. S., Bluhm, H., Mysak, E. R., Smith, J. D., Kolb, C.
1258 E., and Worsnop, D. R.: Carbon oxidation state as a metric for describing the chemistry of
1259 atmospheric organic aerosol, *Nat. Chem.*, 3, 133–139, <https://doi.org/10.1038/nchem.948>, 2011.
- 1260 Kuylenstierna, J. C., Rodhe, H., Cinderby, S., and Hicks, K.: Acidification in developing countries:
1261 ecosystem sensitivity and the critical load approach on a global scale., *Ambio*, 30, 20–28,
1262 <https://doi.org/10.1579/0044-7447-30.1.20>, 2001.
- 1263 Laquer, F. C.: Sequential precipitation samplers: A literature review, *Atmospheric Environ. Part*
1264 *Gen. Top.*, 24, 2289–2297, [https://doi.org/10.1016/0960-1686\(90\)90322-E](https://doi.org/10.1016/0960-1686(90)90322-E), 1990.
- 1265 Laurent, B., Losno, R., Chevaillier, S., Vincent, J., Rouillet, P., Bon Nguyen, E., Ouboulmane, N.,
1266 Triquet, S., Fornier, M., Raimbault, P., and Bergametti, G.: An automatic collector to monitor
1267 insoluble atmospheric deposition: application for mineral dust deposition, *Atmospheric Meas.*
1268 *Tech.*, 8, 2801–2811, <https://doi.org/10.5194/amt-8-2801-2015>, 2015.
- 1269 Lawrence, C. E., Casson, P., Brandt, R., Schwab, J. J., Dukett, J. E., Snyder, P., Yerger, E., Kelting,
1270 D., VandenBoer, T. C., and Lance, S.: Long-term monitoring of cloud water chemistry at
1271 Whiteface Mountain: the emergence of a new chemical regime, *Atmospheric Chem. Phys.*, 23,
1272 1619–1639, <https://doi.org/10.5194/acp-23-1619-2023>, 2023.
- 1273 Likens, G. E. and Butler, T. J.: Atmospheric Acid Deposition, in: *The Handbook of Natural*
1274 *Resources, Atmosphere and Climate*, vol. 6, edited by: Wang, Y., CRC Press, 2020.
- 1275 Lin, W.-C., Brondum, K., Monroe, C. W., and Burns, M. A.: Multifunctional Water Sensors for
1276 pH, ORP, and Conductivity Using Only Microfabricated Platinum Electrodes, *Sensors*, 17,
1277 <https://doi.org/10.3390/s17071655>, 2017.
- 1278 Lindberg, S. E., Lovett, G. M., Richter, D. D., and Johnson, D. W.: Atmospheric Deposition and
1279 Canopy Interactions of Major Ions in a Forest, *Science*, 231, 141–145,
1280 <https://doi.org/10.1126/science.231.4734.141>, 1986.

- 1281 Lovett, G. M.: Atmospheric Deposition of Nutrients and Pollutants in North America: An
1282 Ecological Perspective, *Ecol. Appl.*, 4, 629–650, <https://doi.org/10.2307/1941997>, 1994.
- 1283 Lovett, G. M. and Kinsman, J. D.: Atmospheric pollutant deposition to high-elevation ecosystems,
1284 *Atmospheric Environ. Part Gen. Top.*, 24, 2767–2786, [https://doi.org/10.1016/0960-](https://doi.org/10.1016/0960-1686(90)90164-I)
1285 1686(90)90164-I, 1990.
- 1286 Meteorological Service of Canada: 2004 Canadian Acid Deposition Science Assessment, , Library
1287 and Archives Canada, 2005.
- 1288 Metzger, J. C., Schumacher, J., Lange, M., and Hildebrandt, A.: Neighbourhood and stand
1289 structure affect stemflow generation in a heterogeneous deciduous temperate forest, *Hydrol. Earth*
1290 *Syst. Sci.*, 23, 4433–4452, <https://doi.org/10.5194/hess-23-4433-2019>, 2019.
- 1291 Michalzik, B. and Matzner, E.: Dynamics of dissolved organic nitrogen and carbon in a Central
1292 European Norway spruce ecosystem, *Eur. J. Soil Sci.*, 50, 579–590, [https://doi.org/10.1046/j.1365-](https://doi.org/10.1046/j.1365-2389.1999.00267.x)
1293 2389.1999.00267.x, 1999.
- 1294 Moore, T. R.: Dissolved organic carbon in a northern boreal landscape, *Glob. Biogeochem. Cycles*,
1295 17, <https://doi.org/10.1029/2003GB002050>, 2003.
- 1296 Myers-Pigg, A. N., Louchouart, P., Amon, R. M. W., Prokushkin, A., Pierce, K., and Rubtsov,
1297 A.: Labile pyrogenic dissolved organic carbon in major Siberian Arctic rivers: Implications for
1298 wildfire-stream metabolic linkages, *Geophys. Res. Lett.*, 42, 377–385,
1299 <https://doi.org/10.1002/2014GL062762>, 2015.
- 1300 National Atmospheric Deposition Program: NADP Site Selection and Installation Manual, 2009.
- 1301 Oka, A., Takahashi, J., Endoh, Y., and Seino, T.: Bark Effects on Stemflow Chemistry in a
1302 Japanese Temperate Forest I. The Role of Bark Surface Morphology, *Front. For. Glob. Change*, 4,
1303 <https://doi.org/10.3389/ffgc.2021.654375>, 2021.
- 1304 Pacyna, J. M.: Ecological Processes: Atmospheric Deposition, in: *Encyclopedia of Ecology*, vol.
1305 1, edited by: Jorgensen, S. E. and Fath, B. D., Elsevier Science, 275–285, 2008.
- 1306 Pan, Y., Wang, Y., Xin, J., Tang, G., Song, T., Wang, Y., Li, X., and Wu, F.: Study on dissolved
1307 organic carbon in precipitation in Northern China, *Atmos. Environ.*, 44, 2350–2357,
1308 <https://doi.org/10.1016/j.atmosenv.2010.03.033>, 2010.
- 1309 Peden, M. E., Bachman, S. R., Brennan, C. J., Demir, B., James, K. O., Kaiser, B. W., Lockard, J.
1310 M., Rothery, J. E., Sauer, J., Skowron, L. M., and Slater, M. J.: Methods for collection and analysis
1311 of precipitation, 1986.
- 1312 Pomeroy, J. W., Granger, R., Pietroniro, J., Elliott, J., Toth, B., and Hedstrom, N.: Classification
1313 of the Boreal Forest for Hydrological Processes, in: *Proceedings of the Ninth International Boreal*
1314 *Forest Research Association Conference*, 1999.

- 1315 Pumpanen, J., Lindén, A., Miettinen, H., Kolari, P., Ilvesniemi, H., Mammarella, I., Hari, P.,
1316 Nikinmaa, E., Heinonsalo, J., Bäck, J., Ojala, A., Berninger, F., and Vesala, T.: Precipitation and
1317 net ecosystem exchange are the most important drivers of DOC flux in upland boreal catchments,
1318 *J. Geophys. Res. Biogeosciences*, 119, 1861–1878, <https://doi.org/10.1002/2014JG002705>, 2014.
- 1319 Ramanathan, V. and Carmichael, G.: Global and regional climate changes due to black carbon,
1320 *Nat. Geosci.*, 1, 221–227, <https://doi.org/10.1038/ngeo156>, 2008.
- 1321 Randall, David: *An Introduction to the Global Circulation of the Atmosphere*, Princeton University
1322 Press, Princeton, New Jersey, 43 pp., 2015.
- 1323 Reddy, M. M., Liebermann, T. D., Jelinski, J. C., and Caine, N.: Variation in pH During Summer
1324 Storms Near the Continental Divide in Central Colorado, U.S.A.*, *Arct. Alp. Res.*, 17, 79–88,
1325 <https://doi.org/10.1080/00040851.1985.12004450>, 1985.
- 1326 Richter, D. D. and Lindberg, S. E.: Wet Deposition Estimates from Long-Term Bulk and Event
1327 Wet-Only Samples of Incident Precipitation and Throughfall, *J. Environ. Qual.*, 17, 619–622,
1328 <https://doi.org/10.2134/jeq1988.00472425001700040017x>, 1988.
- 1329 Ryan, K. A., Adler, T., Chalmers, A., Perdrial, J., Shanley, J. B., and Stubbins, A.: Event Scale
1330 Relationships of DOC and TDN Fluxes in Throughfall and Stemflow Diverge From Stream
1331 Exports in a Forested Catchment, *J. Geophys. Res. Biogeosciences*, 126, e2021JG006281,
1332 <https://doi.org/10.1029/2021JG006281>, 2021.
- 1333 Safieddine, S. A. and Heald, C. L.: A Global Assessment of Dissolved Organic Carbon in
1334 Precipitation, *Geophys. Res. Lett.*, 44, 11,672-11,681, <https://doi.org/10.1002/2017GL075270>,
1335 2017.
- 1336 Saleh, R.: From Measurements to Models: Toward Accurate Representation of Brown Carbon in
1337 Climate Calculations, *Curr. Pollut. Rep.*, 6, 90–104, <https://doi.org/10.1007/s40726-020-00139-3>,
1338 2020.
- 1339 Sanei, H., Outridge, P. M., Goodarzi, F., Wang, F., Armstrong, D., Warren, K., and Fishback, L.:
1340 Wet deposition mercury fluxes in the Canadian sub-Arctic and southern Alberta, measured using
1341 an automated precipitation collector adapted to cold regions, *Atmos. Environ.*, 44, 1672–1681,
1342 <https://doi.org/10.1016/j.atmosenv.2010.01.030>, 2010.
- 1343 Santín, C., Doerr, S. H., Kane, E. S., Masiello, C. A., Ohlson, M., de la Rosa, J. M., Preston, C.
1344 M., and Dittmar, T.: Towards a global assessment of pyrogenic carbon from vegetation fires, *Glob.
1345 Change Biol.*, 22, 76–91, <https://doi.org/10.1111/gcb.12985>, 2016.
- 1346 Siksna, R.: The electrolytical conductivity of precipitation water as an aid to the chemical analysis,
1347 *Geofis. Pura E Appl.*, 42, 32–41, <https://doi.org/10.1007/BF02113385>, 1959.
- 1348 Sleutel, S., Vandenbruwane, J., De Schrijver, A., Wuyts, K., Moeskops, B., Verheyen, K., and De
1349 Neve, S.: Patterns of dissolved organic carbon and nitrogen fluxes in deciduous and coniferous
1350 forests under historic high nitrogen deposition, *Biogeosciences*, 6, 2743–2758,
1351 <https://doi.org/10.5194/bg-6-2743-2009>, 2009.

- 1352 Smith, W. H.: *Air Pollution and Forests: Interactions Between Air Contaminants and Forest*
1353 *Ecosystems*, 1st ed., Springer, New York, NY, 379 pp., 1981.
- 1354 Stedman, J. R., Heyes, C. J., and Irwin, J. G.: A comparison of bulk and wet-only precipitation
1355 collectors at rural sites in the United Kingdom, *Water, Air, Soil Pollut.*, 52, 377–395,
1356 <https://doi.org/10.1007/BF00229445>, 1990.
- 1357 Stoddard, J. L., Jeffries, D. S., Lükewille, A., Clair, T. A., Dillon, P. J., Driscoll, C. T., Forsius,
1358 M., Johannessen, M., Kahl, J. S., Kellogg, J. H., Kemp, A., Mannio, J., Monteith, D. T., Murdoch,
1359 P. S., Patrick, S., Rebsdorf, A., Skjelkvåle, B. L., Stainton, M. P., Traaen, T., van Dam, H.,
1360 Webster, K. E., Wieting, J., and Wilander, A.: Regional trends in aquatic recovery from
1361 acidification in North America and Europe, *Nature*, 401, 575–578, <https://doi.org/10.1038/44114>,
1362 1999.
- 1363 Stubbins, A., Silva, L. M., Dittmar, T., and Van Stan, J. T.: Molecular and Optical Properties of
1364 Tree-Derived Dissolved Organic Matter in Throughfall and Stemflow from Live Oaks and Eastern
1365 Red Cedar, *Front. Earth Sci.*, 5, <https://doi.org/10.3389/feart.2017.00022>, 2017.
- 1366 Thornton, M. M., Shrestha, R., Wei, Y., Thornton, P. E., Kao, S.-C., and Wilson, B. E.: Daymet:
1367 Monthly Climate Summaries on a 1-km Grid for North America, Version 4 R1,
1368 <https://doi.org/10.3334/ORNLDAAAC/2131>, 2022.
- 1369 Thornton, P. E., Running, S. W., and White, M. A.: Generating surfaces of daily meteorological
1370 variables over large regions of complex terrain, *Aggreg. Descr. Land-Atmosphere Interact.*, 190,
1371 214–251, [https://doi.org/10.1016/S0022-1694\(96\)03128-9](https://doi.org/10.1016/S0022-1694(96)03128-9), 1997.
- 1372 Thornton, P. E., Shrestha, R., Thornton, M., Kao, S.-C., Wei, Y., and Wilson, B. E.: Gridded daily
1373 weather data for North America with comprehensive uncertainty quantification, *Sci. Data*, 8, 190,
1374 <https://doi.org/10.1038/s41597-021-00973-0>, 2021.
- 1375 United States Environmental Protection Agency: Integrated Science Assessment (ISA) for Oxides
1376 of Nitrogen, Oxides of Sulfur and Particulate Matter Ecological Criteria (Final Report, 2020), U.S.
1377 Environmental Protection Agency, Washington, DC, 2020.
- 1378 Van Stan, J. T. and Stubbins, A.: Tree-DOM: Dissolved organic matter in throughfall and
1379 stemflow, *Limnol. Oceanogr. Lett.*, 3, 199–214, <https://doi.org/10.1002/lol2.10059>, 2018.
- 1380 Van Stan, J. T., Wagner, S., Guillemette, F., Whitetree, A., Lewis, J., Silva, L., and Stubbins, A.:
1381 Temporal Dynamics in the Concentration, Flux, and Optical Properties of Tree-Derived Dissolved
1382 Organic Matter in an Epiphyte-Laden Oak-Cedar Forest, *J. Geophys. Res. Biogeosciences*, 122,
1383 2982–2997, <https://doi.org/10.1002/2017JG004111>, 2017.
- 1384 VandenBoer, T. C.: AIM-IC: Applications to Nitrous Acid (HONO) in the Ambient Atmosphere
1385 and Precipitation Monitoring, Masters of Science, University of Toronto, 2009.
- 1386 Vermette, S. J. and Drake, J. J.: Simplified wet-only and sequential fraction rain collector,
1387 *Atmospheric Environ.* 1967, 21, 715–716, [https://doi.org/10.1016/0004-6981\(87\)90053-9](https://doi.org/10.1016/0004-6981(87)90053-9), 1987.

- 1388 Vet, R., Artz, R. S., Carou, S., Shaw, M., Ro, C.-U., Aas, W., Baker, A., Bowersox, V. C.,
1389 Dentener, F., Galy-Lacaux, C., Hou, A., Pienaar, J. J., Gillett, R., Forti, M. C., Gromov, S., Hara,
1390 H., Khodzher, T., Mahowald, N. M., Nickovic, S., Rao, P. S. P., and Reid, N. W.: A global
1391 assessment of precipitation chemistry and deposition of sulfur, nitrogen, sea salt, base cations,
1392 organic acids, acidity and pH, and phosphorus, *Glob. Assess. Precip. Chem. Depos. Sulfur*
1393 *Nitrogen Sea Salt Base Cations Org. Acids Acidity PH Phosphorus*, 93, 3–100,
1394 <https://doi.org/10.1016/j.atmosenv.2013.10.060>, 2014.
- 1395 Wang, X., Gemayel, R., Baboosian, V. J., Li, K., Boreave, A., Dubois, C., Tomaz, S., Perrier, S.,
1396 Nizkorodov, S. A., and George, C.: Naphthalene-Derived Secondary Organic Aerosols Interfacial
1397 Photosensitizing Properties, *Geophys. Res. Lett.*, 48, e2021GL093465,
1398 <https://doi.org/10.1029/2021GL093465>, 2021.
- 1399 Washenfelder, R. A., Azzarello, L., Ball, K., Brown, S. S., Decker, Z. C. J., Franchin, A.,
1400 Fredrickson, C. D., Hayden, K., Holmes, C. D., Middlebrook, A. M., Palm, B. B., Pierce, R. B.,
1401 Price, D. J., Roberts, J. M., Robinson, M. A., Thornton, J. A., Womack, C. C., and Young, C. J.:
1402 Complexity in the Evolution, Composition, and Spectroscopy of Brown Carbon in Aircraft
1403 Measurements of Wildfire Plumes, *Geophys. Res. Lett.*, 49, e2022GL098951,
1404 <https://doi.org/10.1029/2022GL098951>, 2022.
- 1405 Wetherbee, G. A., Shaw, M. J., Latysh, N. E., Lehmann, C. M. B., and Rothert, J. E.: Comparison
1406 of precipitation chemistry measurements obtained by the Canadian Air and Precipitation
1407 Monitoring Network and National Atmospheric Deposition Program for the period 1995–2004,
1408 *Environ. Monit. Assess.*, 164, 111–132, <https://doi.org/10.1007/s10661-009-0879-8>, 2010.
- 1409 Wonaschütz, A., Hersey, S. P., Sorooshian, A., Craven, J. S., Metcalf, A. R., Flagan, R. C., and
1410 Seinfeld, J. H.: Impact of a large wildfire on water-soluble organic aerosol in a major urban area:
1411 the 2009 Station Fire in Los Angeles County, *Atmospheric Chem. Phys.*, 11, 8257–8270,
1412 <https://doi.org/10.5194/acp-11-8257-2011>, 2011.
- 1413 Ziegler, S. E., Benner, R., Billings, S. A., Edwards, K. A., Philben, M., Zhu, X., and Laganière, J.:
1414 Climate Warming Can Accelerate Carbon Fluxes without Changing Soil Carbon Stocks, *Front.*
1415 *Earth Sci.*, 5, <https://doi.org/10.3389/feart.2017.00002>, 2017.
- 1416